

# **Contrasting mechanisms for crustal sulphur contamination of mafic magma: evidence from dyke and sill complexes from the British Palaeogene Igneous Province**

**Hannah S. R. Hughes<sup>1\*</sup>, Adrian J. Boyce<sup>2</sup>, Iain McDonald<sup>1</sup>, Brett Davidheiser-Kroll<sup>2</sup>, David A. Holwell<sup>3</sup>, Alison McDonald<sup>2</sup>, Anthony Oldroyd<sup>1</sup>,**

<sup>1</sup>School of Earth and Ocean Sciences, Cardiff University, Park Place, Cardiff, CF10 3AT, UK

<sup>2</sup>Scottish Universities Environment Research Centre, Rankine Avenue, East Kilbride, Glasgow, G75 0QF, UK

<sup>3</sup>Department of Geology, University of Leicester, University Road, Leicester, LE1 7RH, UK

\*Corresponding author email: [HughesH6@cf.ac.uk](mailto:HughesH6@cf.ac.uk); Telephone: +44(0)29 208 76420

*Submission to: **Journal of the Geological Society, London***

2

3   **Abstract**

4   The addition of crustal sulphur to magma can trigger sulphide saturation: a process fundamental to  
5   the development of some Ni-Cu-PGE deposits. In the British Palaeogene Igneous Province, mafic and  
6   ultramafic magmas intrude a thick sedimentary sequence offering opportunities to elucidate  
7   mechanisms of magma–crust interaction in a setting with heterogeneous S isotope signatures. We  
8   present S-isotopic data from sills and dykes on the Isle of Skye. Sharp contrasts exist between  
9   variably light  $\delta^{34}\text{S}$  in Jurassic sedimentary sulphide (-35 to -10‰) and a local pristine magmatic  $\delta^{34}\text{S}$   
10   signature of  $-2.3 \pm 1.5\text{‰}$ . Flat-lying sills have restricted  $\delta^{34}\text{S}$  (-5 to 0‰) while steeply dipping dykes  
11   are more variable (-30 to -2‰). We suggest that the mechanism by which magma is intruded exerts  
12   a fundamental control on the degree of crustal contamination by volatile elements. Turbulent flow  
13   within narrow, steep magma conduits, discordant to sediments, and developed by brittle  
14   extension/dilation have maximum contamination potential. In contrast, sill-like conduits emplaced  
15   concordantly to sediments show little contamination by crustal S. The province is prospective for Ni-  
16   Cu-PGE mineralization analogous to the sill-hosted Noril'sk deposit and Cu/Pd ratios of sills and  
17   dykes on Skye indicate that magmas had already reached S-saturation before reaching the present  
18   exposure level.

19

Supplementary material: Supplementary Material (A) provides details of the whole-rock chemical sulphur extraction methodology. Supplementary Material (B) provides simplified geological maps of the Isle of Skye (Geographical Information System shapefiles © Edina Digimaps 05/10/2011), a geological cross-section of part of southern Skye, and a stratigraphic log of the Mesoproterozoic and Mesozoic sediments of western Scotland. Supplementary Material (C) provides trace element diagrams of sills and dykes used in this study. Supplementary Material (D) provides tables for QA/QC of S-isotope results. In addition, Table A gives sample location information, Table B gives whole-rock major and trace element results for sill and dyke samples, and Table C provides whole-rock major and trace element compositions for Jurassic mudrocks. All Supplementary Material is available at [www.geolsoc.org.uk/SUP00000](http://www.geolsoc.org.uk/SUP00000)

Keywords: Sulphur isotopes, British Palaeogene Igneous Province, magma, crustal contamination

The Palaeogene North Atlantic Igneous Province (NAIP) formed from the intrusion and eruption of mantle-sourced magmas, after the impingement of the proto-Icelandic mantle plume onto overlying lithosphere. Continental rifting initiated in the Palaeogene, with an initial phase of magmatism at 62 Ma in the UK, Greenland and Baffin Island, and ultimately led to the opening of the Atlantic Ocean (continental rifting initiated c. 55 Ma; Saunders *et al.*, 1997). The main products of this prolonged period of magmatism were tholeiitic basalts, in addition to alkali basalts. Where the mantle plume impinged on continental areas, magma fractionation, differentiation, and contamination were commonplace.

The Isle of Skye and surrounding Western Isles of Scotland host a number of prominent intrusive and volcanic features of the British Palaeogene Igneous Province (BPIP; Fig. 1a). On Skye, upper crustal mafic and ultramafic intrusions were injected through Archaean Lewisian gneiss basement of the North Atlantic Craton and Mesoproterozoic Torridonian sandstones, siltstones and mudstones. At the current erosion level, the BPIP intrusions (for example the flat-lying Trotternish Sill Complex and an extensive vertical suite of basalt dykes; Fig. 1a) have also penetrated through a thick succession of Mesozoic sedimentary rocks of the Hebrides Basin, which are well exposed and can be demonstrated to be physically contaminating BPIP magmas (e.g., via the presence of xenoliths).

The sulphur content of magma may be dramatically increased during crustal contamination and may exceed the saturation concentration, triggering exsolution of an immiscible sulphide liquid into which chalcophile elements such as Cu, Ni and the PGE may partition (e.g., Naldrett 2004, 2011 and references therein). Magmas that intrude through the Jurassic mudrocks have particular potential for Ni-Cu-PGE mineralization as these sediments would be expected to contain a high level of pyrite with biogenically-derived sulphur (e.g., Fisher & Hudson, 1987). The source of this crustal sulphur can be established by comparing the  $\delta^{34}\text{S}$  signature of the magmas with that of the country rocks through which it has ascended. In crustal sediments, a substantial range of  $\delta^{34}\text{S}$  compositions may be preserved in diagenetic sulphides, mostly pyrite. The sulphide isotopic range arises from mass-

dependent fractionation during bacterial reduction of seawater sulphate in the contemporaneous diagenetic marine environment, which produces sulphide typically  $\leq 20\%$  lighter than the starting sulphate (Ohmoto & Goldhaber, 1997). The range of  $\delta^{34}\text{S}$  can range over 10's of per mille (‰), with Palaeozoic and Mesozoic sulphides extending to more negative values than Precambrian rocks (Canfield & Teske, 1996; Parnell *et al.*, 2010). By contrast, the  $\delta^{34}\text{S}$  signature of the mantle usually ranges from -2 to +2‰, and magmatic signatures can range from -4 to +4‰ depending on the oxidation state of the magma (Ohmoto & Rye, 1979). Due to the dynamic nature of magma intrusion, the crustal S-isotopic signature may be transported away from the immediate site of contamination throughout magma ascent. Therefore crustal S input could be detected remotely from concentrated sulphide mineralization. Such contamination is typically revealed by analysis of S-isotopes in sulphide minerals or whole-rock samples. Our study uses and develops both techniques to test for crustal contamination in the BPIP. The addition of crustal sulphur to a magmatic system is commonly considered essential in the formation of orthomagmatic Ni-Cu-PGE mineralization (e.g., Naldrett 2004, 2011; Ripley & Li, 2013) and hence identifying the controls on crustal sulphur contamination, and where this may be occurring will refine strategies for targeting of Ni-Cu-PGE orthomagmatic mineralization in the BPIP and elsewhere.

We present the first published sulphur isotope compositions for the BPIP, determining a 'framework' for the country rock  $\delta^{34}\text{S}$  of the Hebrides Basin vs.  $\delta^{34}\text{S}$  of the BPIP upper crustal intrusions on Skye (including samples from the Lewisian basement, Torridonian sediments, and various Jurassic sediments of the Hebrides Basin). We identify the 'background' plume magmatic sulphur isotopic composition of the BPIP, and investigate if widespread crustal sulphur contamination of magmas took place in NW Scotland. Coupled with whole-rock Ni, Cu and platinum group element (PGE) concentrations, this contributes towards the development of a new model for magmatic sulphur contamination, dependent on the orientation and energy by which magma is intruded through a conduit, which impacts upon near-field exploration models for orthomagmatic Ni-Cu-PGE deposits.

<< insert Fig. 1 >>

## **1. Geology of the Hebridean portion of the British Palaeogene Igneous Province (BPIP)**

The British Palaeogene Igneous Province (BPIP) is part of the earliest magmatic series of the NAIP, which includes Palaeogene rocks of the Hebridean Igneous Province (along the W coast of Scotland) and Northern Ireland (Fig. 1a). In Scotland, the BPIP includes the Isles of Mull, Skye, Arran, the Small Isles (Rum, Eigg, Muck, Canna and Sanday), together with the mainland igneous complex of Ardnamurchan and lava flows of Morvern. Thus, the BPIP in Scotland extends over a number of tectonic terranes.

Crustal impingement of mantle-sourced mafic magmas resulted in subaerial eruptions along fissure-type feeders (Kent *et al.*, 1998), now seen as a laterally continuous linear array of dyke swarms, with individual dykes typically < 10m wide (Emeleus & Bell, 2005). These NW-SE trending dykes are perpendicular to the North Atlantic rift margin and indicative of the contemporaneous NE-SW directed extension of NW Europe at this time (Emeleus & Bell, 2005). Sills associated with lava fields and central complexes normally occur within Mesozoic sediments below lavas, suggesting a relatively shallow emplacement depth (probably < 1km). Individual sill thicknesses range from up to 10s of metres, amalgamating to form complexes 100s metres in thickness. Sills are often observed to have their own compositional characteristics, unrelated to other overlying lavas. Sills predominantly consist of alkali olivine basalts and tholeiitic basalts, although trachytes and rhyolites are recognised as minor fractionation products (Emeleus & Bell, 2005).

### **1.1 Palaeogene geology of the Isle of Skye**

The Isle of Skye records numerous exposures of BPIP magmatic rocks injecting through and into a thick Mesozoic sedimentary sequence, part of the Hebrides Basin (Harker, 1904). Below the Mesozoic rocks, a thick crustal pile of deformed Neoproterozoic (Torridon and Sleaf Group)

sediments are present above Archaean (Lewisian) basement (Fig. 1b). Hence the Isle of Skye provides an excellent opportunity to study the sources, extent and controls on crustal sulphur contamination in a continental rift environment.

#### **1.1.1 The Trotternish Sill Complex, northern Skye**

The Trotternish Sill Complex outcrops on the Trotternish Peninsula on the north of the Isle of Skye intruding Jurassic sandstones, limestones and marls (Fig. 1a; Gibb & Gibson, 1989). The picrites, picrodolerites, and crinanites (analcite olivine dolerites) present throughout the sill complex are genetically related, and thought to result from differentiation of an alkali-olivine basalt magma (Gibson & Jones, 1991) with varying crustal contamination (Simkin, 1967; Gibson, 1990). This horizontal sill complex post-dates the Skye Lava Group and is at least 250m thick, with individual sills measuring 10's of metres in thickness. Rafts or 'packages' of Jurassic sediments (now baked) occur sporadically within the thickness of the Trotternish Sill Complex in various locations. Sills can display multiple and composite lithologies or melt generations, with banding commonplace (Gibson & Jones, 1991; Emeleus & Bell, 2005). In these cases, the lower zones of a sill are the most mafic. For a detailed 'stratigraphy' of the Trotternish Sill Complex, the reader is referred to Gibson (1990) and Gibson & Jones (1991).

#### **1.1.2 Dykes from the Robustan area of the Strathaird Peninsula, southern Skye**

Dyke swarms on the Isle of Skye are predominantly directed in a NW-SE azimuth and caused significant local crustal dilation. Most dykes are < 1 m thick, but some wider dykes (e.g., Strathaird Peninsula) display evidence of incremental build-up due to multiple mafic magma injections, resulting in magma mingling and layering within dykes (Platten, 2000). The Skye Dyke Swarm intrudes both lavas and gabbros of the Cuillin Centre, and are mutually cut by cone-sheets (Bell & Williamson, 2002). Compositionally, the Skye Dyke Swarm ranges from silicic pitchstones, to alkali

and tholeiitic basalts, and trachytes (Emeleus & Bell, 2005). Ultramafic dykes are predominantly found closest to the Cuillin Central Complex.

At Robustan on the Strathaird Peninsula, southern Isle of Skye (see Fig. 1a), abundant NNW-SSE to NW-SE trending basaltic dykes (hereafter called “Robustan dykes”) cross-cut both the lavas and sediments (see cross-section, Fig. 2). They represent part of a larger dyke swarm, formed and intruded after the eruption of the Strathaird lavas, and after the intrusion of the Cuillin Central Complexes to the N and NW. The cross-section in Figure 2 displays the transect from which dyke and sediment samples were collected. Rare or minor examples of more evolved dyke compositions are also observed, including basaltic trachyandesites. The dykes are typically vertical and range from 30 cm to 10 m in width. The dykes are finely crystalline (crystal size < 1mm) and equigranular. Chilled margins are usually absent.

<< insert Fig. 2 >>

## **2. Stratigraphy of the Hebrides Basin and potential for crustal S contamination**

The Mesoproterozoic Torridonian succession of NW Scotland (Fig. 1b) divides into the Sleat, Stoer and Torridon Groups. It is dominated by sandstones and psammites (Stewart, 2002; Kinnaird *et al.*, 2007). Minor siltstone and mudrock units are thinner and less extensive than in the overlying Jurassic units. Recent sulfur isotope studies of Torridonian sulphates and sulphides from the far NW of Scotland (Stoer to Gruinard Bay) have identified an isotopic shift in  $\delta^{34}\text{S}$  associated with bacterial sulphate reduction, highlighting that the Mesoproterozoic terrestrial environment was adequately oxygenated to support life (Parnell *et al.*, 2010; Parnell *et al.*, 2012). For example, pyrite-bearing lacustrine siltstones of the Diabaig Formation (basal Torridonian) have  $\delta^{34}\text{S}$  compositions of  $-30.1 \pm 17.3$  ‰. During the present study, 14 Torridonian, Sleat, and Stoer Group sediment samples were collected from the Isle of Skye and Rum for sulphur isotopic analysis. Of these, only 5 samples



yielded enough sulphide precipitate (following whole-rock sulphur extraction – see Section 3.2) to allow for conventional S isotope analysis.

The anticipated sulphur concentration of the Lewisian crystalline basement and Mesoproterozoic sediments is significantly lower than in the Mesozoic Hebrides Basin, so while the S-isotopic composition of all of these potential contaminants was analysed during this study, the main focus is laid on the Mesozoic. The sedimentary stratigraphy of the Mesozoic Hebrides Basin is presented in Figure 1b (based on Morton & Hudson, 1995; Hesselbo & Coe, 2000). While several literature sources document the carbon and oxygen isotopic composition of these rocks, only Yallup *et al.* (2013) report the sulphur isotopic composition of a single unit (in the Middle Jurassic Cullaidh Shale Formation; mean bulk rock  $\delta^{34}\text{S}$   $-0.7 \pm 1.8$ ). Sulphur isotopes for Jurassic sediments from elsewhere in the British Isles have been reported (e.g., Raiswell *et al.*, 1993; Hudson *et al.*, 2001) however until now there has been no Hebridean ‘stratigraphy’ of sulphur isotopes available in order to establish a S-isotope framework of potential contaminants to BPIP magmas. In the present study, the Palaeogene igneous rocks of interest are observed intruding through, and physically being contaminated by Jurassic sedimentary sequences (via the presence of xenoliths). Thus, it is specifically the Jurassic units which are of most interest for the purposes of this study. This is due to the high proportion and volume of S-rich shales and mudrocks throughout this Jurassic succession, unlike in the older Triassic, or younger Cretaceous sediments that are sulphur poor and sporadically developed across the region (e.g., Hesselbo & Coe, 2000).

The Trotternish Sills intrude through the same thick package of Jurassic sediments as the Robustan dykes on the Strathaird Peninsula. Thus equivalent Jurassic sedimentary rocks are present as potential contaminants to ascending BPIP magmas and allow for the two different types of intrusive body (sill vs. dyke) to be tested against one another for their degree of crustal S contamination.

### 3. Methodology

#### 3.1 Sampling strategy

In northern Skye, 23 Trotternish Sill Complex samples were collected, including a range of all rock types (picrites, picrodolerites, and crinanites – see Supplementary Tables). Of these, 11 samples were analysed for sulphur isotopes, and PGE and Au.

At Lealt Quarry [NG 5188 6064], a finely crystalline dyke (crystals < 0.5 mm) approximately 2m wide (strike 338°) with a vertical orientation cuts the Trotternish Sill Complex (comprising an upper crinanite sill, overlying a picrite sill and pegmatitic picrite sill – Fig. 3a). The dyke contains 2-20cm centimetre-scale elongate xenoliths of a baked mudrock (likely of Jurassic origin) and 5-10cm picrite sill xenoliths at its margins (Fig. 3b). The dyke appears to be compound with faint vertical banding (showing indistinct boundaries) at its centre, and elongate xenolith trails within some bands (Fig. 3c). This indicates multiple injections of basalt in the dilatational fracture through which the dyke has intruded. Disseminated millimetre-scale (2-10mm) pyrite crystals are associated with these xenoliths and at the dyke margins, with most disseminated pyrite mineralization at the contacts with mudrock xenoliths, or forming 'stringers' through the basalt dyke within 30cm of the xenoliths. There are also trails of white-coloured zeolites (2-10mm diameter) within 20cm of the dyke margin (Fig. 3d). Four samples from the Lealt Quarry basaltic dyke, which cross-cuts the sill units and four Jurassic sediment samples from packages adjacent to or within the Trotternish Sill Complex, were also collected from northern Skye (e.g. Fig. 3e).

In southern Skye, 1 basaltic trachyandesite and 8 basaltic dyke samples were collected from a NW-SE oriented transect approximately 1 km in length through the Jurassic succession at Robustan (Fig. 2). All dykes ranged between 30 cm and 8 m in width, with most measuring 1 – 2.5 m wide. One dyke

(SK51) displayed rare quartz-filled amygdales up to 0.5cm in diameter, however all other sampled dykes were amygdale-free. Dyke samples SK124 and SK129 contained visible pyrite within 5cm of the dyke contact with sediments. Samples were collected from a mixture of dyke margins and central zones. In southern Skye, 5 samples of the Jurassic sediments were collected from this area, including shales, a siltstone, and sandstones.

<< insert Fig. 3 >>

<< insert Table 1 >>

### 3.2. Whole-rock geochemistry

Major and trace element analyses (including PGE and Au) and S isotopic ( $\delta^{34}\text{S}$ ) results are given in Table 1 respectively. A selection of igneous and sedimentary samples were also analysed for elemental S abundance. Sediment S isotopic compositions and S concentrations, spanning the upper portion of the Lower to the Upper Jurassic, are presented in Table 1, and a sub-selection of 4 sediments were analysed for their major and trace element geochemistry (Supplementary Material). For the Lower Jurassic, samples were obtained from outcrops on the Ardnamurchan Peninsula, mainland Scotland. In addition, we analysed the S-isotopic composition of 2 sulphide-bearing samples from the Lewisian gneisses of NW Scotland (X66 and X11b), and 1 sample of Moine metapelite from Ardnamurchan (AN78 – Table 1).

Unweathered material was crushed, split, and milled to a fine powder in an agate planetary ball mill. Major and trace elements were analysed by inductively coupled plasma optical emission spectrometry (ICP-OES – JY Horiba Ultima-2) and inductively coupled plasma mass spectrometry (ICP-MS - Thermo X Series 2) respectively at Cardiff University using methods and instrumentation described by McDonald & Viljoen (2006). Platinum Group Element (PGE) and Au analysis for samples was carried out by Ni-sulphide fire assay followed by Te co-precipitation and ICP-MS (Huber *et al.*,

2000; McDonald & Viljoen, 2006). Accuracy for whole-rock elemental geochemistry was constrained by analysis of the certified reference materials TDB1 and WMG1 for PGE and Au, and JB1a for all other trace and major elements (Supplementary Material). Precision was determined by repeat analysis of a sub-set of samples, with most elements repeatable to within 10% or better.

### 3.3. Sulphur isotope analyses

Samples with visible sulphide minerals  $>500\mu\text{m}^2$  were cut into blocks (up to 40 x 20 mm in area) and polished. *In-situ* laser combustion of polished sulphides was carried out following the technique of (Wagner *et al.*, 2002). Based on experimental results, laser combustion causes a small and predictable fractionation of sulphur isotope compositions for  $\delta^{34}\text{S}$  of the  $\text{SO}_2$  gas produced, compared to the actual  $\delta^{34}\text{S}$  of the sulphide mineral (Wagner *et al.*, 2002). Therefore the raw  $\delta^{34}\text{S}$  data were corrected by the following factor:  $\delta^{34}\text{S}_{\text{pyrite}} = \delta^{34}\text{S}_{\text{SO}_2\text{laser}} + 0.8\text{‰}$ . Whole-rock S extracted from the rocks (see below), and a series of samples from which sulphide separates could be picked, were analysed following the technique of Robinson & Kusakabe (1975).

$\text{SO}_2$  gas samples were analysed at the Scottish Universities Environment Research Centre (SUERC) using a ThermoFisher Scientific MAT 253 dual inlet mass spectrometer (for conventional samples) and an on-line VG Isotech SIRA II mass spectrometer (for laser combustion samples). Standards used throughout all analyses were IAEA-S-3 and NBS-123 international standards, alongside an SUERC laboratory chalcopyrite standard, CP-1. The results for these gave  $-31.5\text{‰}$  (IAEA-S-3, certified to be  $-31.5\text{‰}$ ),  $-4.5\text{‰}$  (CP-1, certified  $-4.6\text{‰}$ ) and  $+17.1\text{‰}$  (NBS-123; certified  $+17.1\text{‰}$ ), with  $2\sigma < \pm 0.2\text{‰}$  reproducibility, based on repeated standard analyses. All data are reported in standard per-mille variations from the Vienna Cañon Diablo troilite standard, V-CDT. Full analytical run details can be found in the Supplementary Material.

Our Chromium Reducible Sulphur (CRS) sulphide extraction procedure (for whole-rock powders) is based on and adapted from numerous published and unpublished procedures (Zhabina & Volkov,

1978; Canfield *et al.*, 1986; Tuttle *et al.*, 1986; Hall *et al.*, 1988; Newton *et al.*, 1995; Nielsen & Hanken, 2002; Labidi *et al.*, 2012). A diagram and written description for the procedure can be found in the Supplementary Material.

### 3.4. Whole-rock sulphur concentration analysis

A selection of powdered rock samples were analysed for bulk rock S concentration by LECO CS230 Carbon/Sulphur Determinator at the University of Leicester, UK. Between 0.1 and 1.0 g of sample were used depending on relative bulk S content. Samples were ignited in an O<sub>2</sub> stream and the SO<sub>2</sub> produced was analysed by infra-red absorption. Each sample was run in triplicate to monitor precision. Accuracy was monitored by regular analysis of the reference material BAS ECRM 877-1. The limit of minimum detection for this method is 0.018 wt.% S, which is calculated based on 3 x standard deviation of the mean blank value. A total of 11 samples (both BPIP intrusives and sedimentary rocks) were analysed by this method.

## 4. Results of $\delta^{34}\text{S}$ and S determinations

### 4.1 Trotternish Sill Complex

The  $\delta^{34}\text{S}$  of the Trotternish Sill Complex (including samples from the chilled margins at the base of the sill complex) ranges from +0.1 to -4.9‰, however sample SK102 from 2m above the base of the complex at Skudiburgh, gave -10.8‰ (Fig. 4). Excluding sample SK102, the mean  $\delta^{34}\text{S}$  of the Trotternish Sills is  $-2.3 \pm 1.5\text{‰}$ . Total PGE concentrations for these sills ranges from 12.6 to 30.9 ppb with no clear correlation between whole-rock total PGE content and whole-rock  $\delta^{34}\text{S}$ . Whole-rock Pd concentration ranges from 2.1 to 10.2 ppb and Cu from 57 to 252 ppm (Fig. 5). The Cu/Pd ratio varies from 13300 to 46200 with two anomalously high ratios of 72800 and 81100 (samples SK89 and SK83, respectively – SK83 is from the base of the picrite sill complex at Dunflodigarry,  $\delta^{34}\text{S} = -4.9\text{‰}$ ). Pd/Ir ratio ranges from 3.1 to 14.1 with an anomalous value of 56.5 for sample SK90 (a

pegmatitic pircite sill from Lealt Quarry,  $\delta^{34}\text{S} = -2.2\text{‰}$ ). Overall, Pt/Pd ratio for the sills varies from 0.94 to 2.55.

The basaltic dyke at Lealt Quarry, which cross-cuts the Trotternish Sill Complex (Fig. 3a and b), has a  $\delta^{34}\text{S}$  of  $-7.5\text{‰}$  at the margins (Fig. 4a), where the dyke has entrained baked mudrock xenoliths ( $\delta^{34}\text{S}$  signature of  $-15.4\text{‰}$ ; Fig. 6). At the centre of the dyke, where xenoliths are absent, the basalt has  $\delta^{34}\text{S} = -6.5\text{‰}$ . At the dyke margin, the total whole-rock PGE concentration is 17.9 ppb, as opposed to 1.18 ppb at the dyke centre. Cu/Pd ratio at the margin is 18650 but is significantly higher in the centre of the dyke (77800). Pt/Pd and Pd/Ir show little variance from the dyke margin to its centre, ranging 12.1 to 14.1, and 1.02 to 1.35 respectively.

<< insert Fig. 4 >>

#### **4.2 Robustan dyke swarm**

The  $\delta^{34}\text{S}$  of 8 samples of basaltic dykes from Robustan ranges from  $-2.3$  to  $-30.7\text{‰}$  (Table 1, Fig. 4a). Sample SK131 (from the centre of a 30cm wide basalt dyke) gave the lightest  $\delta^{34}\text{S}$ , at  $-30.7\text{‰}$ , and has a measured whole-rock sulphur concentration of 1.339 wt.%. Sample SK129 (from the centre of an 80cm wide basalt dyke) gave 0.408 wt.% S and  $-15.5\text{‰}$ , and SK127 (from the centre of a 2.5m wide dyke) has 0.122 wt.% S and  $-5.1\text{‰}$ . This distribution of S isotope composition and S concentration, indicates a strong correlation between the S-isotope signature and concentration of S in the dykes (Fig. 4b) – dykes with a higher concentration of S having significantly lower  $\delta^{34}\text{S}$  (correlation  $r^2 = 0.98$ ). A basaltic trachyandesite, SK130, with approximately 1 mm diameter rounded pyrite crystallised in some portions of the dyke (mostly at the margins) produced  $\delta^{34}\text{S}$  of  $-19.8 \pm 1.4\text{‰}$ .

Total whole-rock PGE concentrations in the dykes range from 6.4 to 52.4 ppb, and Pd ranges from 1.25 to 16.2 ppb (Fig. 5a). Cu concentration ranges from 90.3 to 207 ppm (Fig. 5b). Cu/Pd ratios vary between 5590 and 167200. Pd/Ir varies from 11.9 to 48.8 and Pt/Pd ratio ranges from 0.74 to 2.20.

The Cu/Pd and Pt/Pd ratios of the dykes are chiefly controlled by Pd concentration (Fig. 5c-d). Transposing all samples onto a NW-SE oriented section (Figs. 2 & 5) we observe that the  $\delta^{34}\text{S}$  composition of the dykes becomes significantly lighter from SE to NW. This broadly coincides with an increase in the stratigraphic level of the Jurassic sediments that the dykes cross-cut, and into which they intrude. Arranging the results in this manner, we see that between samples SK126 and SK131 a sharp decrease in Pd concentration coincides with a considerable shift in  $\delta^{34}\text{S}$  (from -2.9 to -30.7‰ respectively) and a sharp rise in Cu/Pd (Fig. 5c). Pt/Pd broadly follows this increasing Cu/Pd trend from SE to NW (Fig. 5d), however SK126 is anomalous due to the significantly higher Pt concentration (25.1 ppb) in this sample.

<< insert Fig. 5 >>

#### **4.3 Sedimentary and contaminant country rock units**

Of the Jurassic sediments collected from Robustan (Fig. 2) and analysed by whole-rock sulphur extraction and conventional analysis, the shale member of the Staffin Shale Formation and the Staffin Bay Formation Carn Mor Sandstone Member have the lightest sulphur isotopic signature, with  $\delta^{34}\text{S} = -32.6$  and  $-33.8$ ‰ respectively (Table 1, Fig. 6). The measured sulphur concentration of the shale was 1130 ppm S, but the concentration of sulphur in the sandstone was below detection limit ( $< 180$  ppm). A siltstone member of the Staffin Shale Formation also yielded an average  $\delta^{34}\text{S} = -29.2$ ‰. As previously mentioned, the assumed Jurassic mudrock xenolith in the Lealt Quarry basalt dyke, produced  $\delta^{34}\text{S} = -15.4$ ‰. Samples of the Staffin Shale Formation (SK103) and Kilmaluag Formation marl (SK108) have very low concentrations of sulphur. Similarly low/absent S contents were recorded in Duntulm Formation limestone. A recrystallized mudstone (Portree Shale Formation) and 2 ironstone samples (Raasay Ironstone Formation with abundant pyrite nodules) from Ardnamurchan produced  $\delta^{34}\text{S} = -17.6$ ‰ and  $-14.7$ ‰ respectively. The pyrite-rich nodules themselves had  $\delta^{34}\text{S} = -18.4$ ‰ but had the highest concentration of S with up to 28 wt.% (Table 1).

The two pyrite-bearing samples of Lewisian amphibolite gneiss collected from the Assynt Terrane in NW Scotland gave a  $\delta^{34}\text{S}$  of -1.4 to +1.2‰. The Moine metapelite from the Ardnurchan Peninsula produced  $\delta^{34}\text{S} = +2.5\text{‰}$ . Torridon and Sleat Mesoproterozoic sediments collected from the Isles of Skye and Rum (Fig. 6a) have  $\delta^{34}\text{S}$  ranging +1.4 to +4.7‰, although few samples out of the total number collected had sufficient S to produce a useable whole-rock  $\text{Ag}_2\text{S}$  precipitate. Samples from the Aultbea Formation sandstone and a shale from the Diabaig Formation were S poor and did not yield sufficient precipitate for analysis. Together with the Archaean Lewisian gneisses and Moine metasediments, the Mesoproterozoic lithologies delineate a limited range of  $\delta^{34}\text{S}$ , from -1.4 to +4.7‰, with a mean of  $+2.0 \pm 1.8\text{‰}$ . This is clearly distinct from the mean Jurassic sediment  $\delta^{34}\text{S}$  of  $-21.5 \pm 8.0\text{‰}$  (e.g., Fig. 6) and offers the potential to act as a tracer of upper shallow crustal contamination in the BPIP intrusive suites.

<< insert Fig. 6 >>

## 5. Discussion

The results of this study provide the first comprehensive S isotope framework for the BPIP through determining the regional crustal signatures and those of the BPIP magmas on Skye. Our work has identified the following key features:

1. Local Precambrian basement has a limited range of  $\delta^{34}\text{S}$  values (-1.4 to +4.7‰) with a mean of  $+2.0 \pm 1.6 \text{‰}$ , which overlaps typical magmatic values. This contrasts markedly with the Mesoproterozoic values found on the mainland by Parnell et al (2010).
2. Local Jurassic sediments have a distinct light  $\delta^{34}\text{S}$  signature ranging -35 to -10 ‰ and a mean of  $-21.5 \pm 8.0\text{‰}$ .



3. The flat-lying intrusions of the Trotternish sill complex intruded into Jurassic sediments have restricted  $\delta^{34}\text{S}$  signatures of -5 to 0 ‰ (with one outlier of -10.8‰).
4. The late vertical Robustan dykes *cross-cutting the same Jurassic units* have much lighter  $\delta^{34}\text{S}$  ranging from -30 to -2 ‰.

Thus the data show that the potential contaminants of the BPIP intrusive rocks on Skye have distinct S isotope signatures, and our study has identified differences in S isotope signature between different styles of intrusion. This provides insights into the sources of S, including local mantle and crustal signatures, and to shed light on models for emplacement and contamination in these intrusives. These aspects are explored in detail below.

### 5.1. What is the value of the local mantle S isotope signature in the BPIP?

Several studies of the sulphur isotopic composition of oceanic basalts have previously been conducted (Kusakabe *et al.*, 1990; Alt *et al.*, 1993; Labidi *et al.*, 2012). Most recently, the reappraisal of MORB  $\delta^{34}\text{S}$  by Labidi *et al.* (2012) indicated that the mantle has a mean value around  $-1 \pm 0.5$  ‰. The sulphur content of such basalts is usually coupled with Fe, Ni and Cu, and is either found within sulphides or dissolved in the silicate melt. At magmatic temperatures, fractionation between the dissolved and segregated sulphide fractions of these basalts would be negligible and the bulk system reduced (Ohmoto & Rye, 1979; Labidi *et al.*, 2012).  $\delta^{34}\text{S}$  of MORB and primary plume-derived magmas can thus be anticipated to broadly represent the  $\delta^{34}\text{S}$  of the local mantle, particularly for primitive high-MgO magmatic rocks, where sulphur exsolution is assumed to be minimal, and contamination *en route* from the mantle likely to be limited (e.g., Iceland).

S isotope analysis of Icelandic basalts show  $\delta^{34}\text{S}$  from -2.0‰ to +0.4‰, with a mean of -0.8‰ (Torssander, 1989). Both tholeiitic and alkaline basalts displayed similar isotopic compositions, although intermediate and acid rocks extend to heavier  $\delta^{34}\text{S}$ , up to +4.2‰. For the Icelandic alkaline and tholeiitic samples of Torssander (1989), the homogeneity of the  $\delta^{34}\text{S}$  distribution provides strong

evidence that the sulphur isotopic composition of the parental magmas had not changed significantly from the mantle source to crustal emplacement.

The mean  $\delta^{34}\text{S}$  of the Trotternish Sills (excluding one anomalously light sample, SK102) is  $-2.3\text{‰} \pm 1.5$ , which is comparable to the signature of basalts from the Iceland plume (Torssander, 1989) and MORB (Labidi *et al.*, 2012), although the range of sulphur isotopic compositions is somewhat larger. Therefore we have confidence that the picritic Trotternish Sill Complex is representative of the mantle S isotopic signature of the plume in this portion of the NAIP and BPIP.

<< insert Fig. 7 >>

## 5.2. Crustal sulphur contamination in dykes from southern Skye

The sulphur isotopic composition and sulphur concentration for the basaltic Robustan dykes (SK127, SK129 and SK131) indicate that the magmas which formed these intrusions were contaminated by crustally-derived sulphur with an isotopically light  $\delta^{34}\text{S}$  signature. Assuming contamination is dominated by the Jurassic rocks a simple binary mixing model may be used, as follows:

$$\delta^{34}\text{S}_{\text{mix}} = [(\delta^{34}\text{S}_{\text{C}} \cdot X_{\text{C}} \cdot f) + (\delta^{34}\text{S}_{\text{M}} \cdot X_{\text{M}} \cdot (1-f))] / [(X_{\text{C}} \cdot f) + (X_{\text{M}} \cdot (1-f))] \quad (\text{equation 1})$$

where the contaminated magma =  $\delta^{34}\text{S}_{\text{mix}}$ ; the isotopic composition of the uncontaminated magma and contaminating sediment =  $\delta^{34}\text{S}_{\text{M}}$  and  $\delta^{34}\text{S}_{\text{C}}$  respectively; the concentration of sulphur in the uncontaminated magma and contaminating sediment =  $X_{\text{M}}$  and  $X_{\text{C}}$  respectively; and the fractional abundance of the contaminant mixing with the magma =  $f$ .

Figure 7 shows a simple binary mixing model for  $\delta^{34}\text{S}$  between an uncontaminated mantle melt and Jurassic sediments (SK50 and SK53). Assuming the  $\delta^{34}\text{S}$  of the contaminant is similar to siltstone SK50, for dyke samples SK126 and SK127, between 2 and 4% input from the sediment S reservoir would account for the measured  $\delta^{34}\text{S}$  in these dykes; whereas for SK129 ( $\delta^{34}\text{S} = -15.5\text{‰}$ ), 17% contamination is required.

For sample SK131, the  $\delta^{34}\text{S}$  of the contaminated dyke is calculable by accounting for 78% of the sulphur isotopic signature as coming from a contaminant (e.g., SK50). Sample SK131 was taken from a 30cm wide basalt dyke. While the field evidence, and whole-rock major and trace element geochemistry indicate that it is likely to be related to the other dyke samples from this area (with the exception of the basalt trachyandesite SK130), the S concentration of this dyke is not representative of the parental magma composition which fed the other Robustan dykes and intruded through neighbouring conduits. Local sulphur concentration could likely be extremely variable in the dykes, particularly if physical entrainment of crustal material is considered. Further, the sulphur concentration within the Jurassic sediments is extremely variable (e.g., sandstone vs. pyrite nodule rich shale). Therefore, as the dykes were intruded through the Jurassic sediment package, they could have experienced contamination by each S-rich horizon in turn as the dyke intruded upwards.

Although we cannot eliminate the possibility of multi-component progressive contamination having taken place in the parental magmas of the dykes during ascent, we can use a mass balance calculation to interpret the maximum contamination scenario. Assuming an initial concentration of 250 ppm sulphur in the parental basaltic magma (based on primitive mantle concentrations; McDonough & Sun, 1995) for a volume of  $1\text{m}^3$  of magma in a  $1\text{m} \times 1\text{m} \times 1\text{m}$  conduit with a 10cm wide baked margin in the wall rocks either side (equivalent to  $0.2\text{m}^3$  wall rock volume and based on visible field evidence) the concentration of sulphur in the wall rock would need to be approximately 7.6 wt.%, assuming a density of  $3000\text{kgm}^{-3}$  and  $2600\text{kgm}^{-3}$  for the basalt and shale respectively. This concentration is considerably higher than that measured in SK50 (1130 ppm). Assuming that the entire sedimentary S budget is accommodated within pyrite, this is equivalent to a shale containing 14% pyrite. Given that pyrite-nodules are recorded within the Jurassic sediment pile of the Hebrides Basin, with 27.7 wt.% S (e.g., sample AN71; Table 1) this is a feasible composition for the contaminant of SK131. Thus, our model can readily accommodate the observed dyke S concentrations and  $\delta^{34}\text{S}$  if the high variability of S concentration in Jurassic shales and ironstones is taken into consideration. Dyke SK131 could have intruded through an isotopically light, pyrite-rich

portion of the sedimentary pile with unusually higher S concentrations than the surrounding shales, thus dramatically reducing the volume of country rock required to be contaminating the magma conduit and accounting for the S-signature of the dyke.

### **5.3. Contrasting S isotope signatures of sills and dykes on Skye**

This study has presented two examples of high-level intrusions from the BPIP and shows that the dykes have incorporated substantial proportions of Jurassic S in both study areas on the Strathaird and Trotternish Peninsulas (e.g., Lealt Quarry). In stark contrast, the sills of the Trotternish Sill Complex display limited sedimentary S contamination, even at the chilled sill margins. Therefore we have a dichotomy – crustally derived sulphur (with a characteristically light isotopic signature) is widely available in high concentrations within the country rocks of both areas, yet other factors appear to control whether or not this is mobilised or preserved in the local magmatic intrusions.

The possibility of post-magmatic sulphur mobility must be considered – is the sulphur signature observed in the dykes a feature of contamination during the magmatic event, or has this been imparted post-emplacement via *in situ* bacterial reduction in the basalts themselves, within fractures, or by low-temperature fluid remobilisation? At Strathaird, the dykes are volumetrically small, and surrounded by isotopically light sulphur-bearing sediments. It is plausible that post-emplacement fluids could have circulated through these sediments and through the dykes, imparting the sedimentary  $\delta^{34}\text{S}$  in this manner. However, textural diagnosis for the timing of sulphide mineral formation might be a better indicator. Where present, pyrite forms subhedral crystals up to 2mm in diameter, typically within 20cm of the dyke margin, and less common at dyke centres, although as highlighted above, this has not precluded the light whole-rock  $\delta^{34}\text{S}$  signature from penetrating the dyke centres. As far as can be determined, there are no veinlets or stringers observed connecting these. In hand specimens, there is no correlation between the presence of oxidised fractures and pyrite, and oxidised/weathered material along with any vugs/amygdales was deliberately removed from the sample before sulphur extraction and analysis. Surface

contamination from overlying peat bogs is a feature of the geography of both the dyke and sill areas, and therefore is unlikely to be a realistic modern source of S to one, and not the other. Therefore at Strathaird, there is no reasonable evidence to presume that the sulphide signature is not a 'primary' feature.

Lastly, we can demonstrate physical evidence of high-level crustal contamination by sedimentary rocks taking place in BPIP magmatic intrusions. The vertical basalt dyke at Lealt Quarry, Trotternish Peninsula, is observed in outcrop intruding through the horizontal picritic Trotternish Sills (Fig. 3a). 50-80m below this quarry, the sills overlie the Jurassic Lealt Shale Formation and it is assumed that the vertical basalt dyke extends through the sills and into the sedimentary pile below it. Field evidence of contamination comes from the centimetre-scale mudrock xenoliths entrained and preserved at the dyke margin (Fig. 3b-d). Pyrite crystals (up to several millimetres in diameter) nucleate within the basalt at the xenolith margins and the xenoliths themselves contain minor pyrite (mostly at the xenolith margins). The  $\delta^{34}\text{S}$  of Trotternish Sills at Lealt Quarry are -2.2 and -1.7‰ (SK90 and SK92). Critically, this demonstrates that it would not be possible to impart the light sulphur isotopic signature observed in the dyke from sulphur present in the host picritic sills. The mudrock xenoliths, although baked and with no characteristically distinguishing features, are undoubtedly from the Jurassic strata, possibly the Lealt Shale Formation or similar lithology, below the current level of exposure. The  $\delta^{34}\text{S}$  of pyrite within the dyke at its margin is -7.5‰, while the whole-rock sulphur signature of the dyke centre is -6.5‰. The whole-rock sulphur signature of a mudrock xenolith is -15.4‰, suggesting that the light  $\delta^{34}\text{S}$  of the dyke has been imparted from Jurassic mudrocks during dyke intrusion and ascent, and involved their physical attrition and brecciation. Accordingly the intact wall rocks to the dyke were baked and chemically interacted with the intruding magma. This is analogous to the dykes on the Strathaird Peninsula, although xenoliths were not observed here, and is in complete contrast to the Trotternish Sills surrounding this dyke exposure.

Mass-independent sulphur diffusion profiles between the Platreef of the Bushveld Complex and footwall country rocks showed that the  $\Delta^{33}\text{S}$  isotopic ratio is particularly sensitive to wall rock sulphur interaction (Penniston-Dorland *et al.*, 2008). For example, the  $\Delta^{33}\text{S}$  profile indicates enrichment of S at the Platreef footwall contact via back diffusion controlled by fluids emanating from the cooling and crystallising magma. This process appears to be limited to 5m inside the igneous contact, however the diffusive and advective distances into the country rocks ranges from 6 to 9m and 16 to 27m respectively (Penniston-Dorland *et al.*, 2008). In the Lealt Quarry dyke, it is unsurprising therefore, that we observe the margins of the dyke to have a stronger sulphur contamination signature than at the centre, as this is where most magma-sediment interaction and element transfer was taking place during intrusion. Further, we demonstrate that it is highly unlikely that the sulphur isotopic signature of the dyke has been imparted post-emplacement by low-temperature fluids from the immediately surrounding host rocks, as the host rocks are picrite sills with a 'magmatic'  $\delta^{34}\text{S}$  and are therefore not isotopically light enough to impart the  $\delta^{34}\text{S}$  found in the basalt dyke.

We have established that the strongly negative  $\delta^{34}\text{S}$  observed in the Skye dykes is a characteristic feature of the magmatic intrusions, inherited from Jurassic sedimentary pyrite with a bacteriogenic  $\delta^{34}\text{S}$  signature, during the magmatic stage. The question arises, why is this signature so rare or absent in the Trotternish Sills? Is there an intrinsic difference between the sills and dykes and their capacity for local, high-level crustal contamination? After all, the sills and the dykes intrude through the same package of sediments on the Strathaird Peninsula as they do on the Trotternish Peninsula. And if contamination is taking place, is it wholesale melting/contamination (with inputs of all elements within the sediment being mixed with the magma), or is there preferential mobilisation of only the most volatile elements like sulphur?

### 5.3.1 The role of emplacement mechanism on the crustal contamination signature

During intrusion, many mechanisms can control the upwards movement of magmas through the crust. These include zone melting, penetrative intrusion, and stoping (Oxburgh *et al.*, 1984). The physical method by which a magma body is emplaced could affect the degree of contamination that results. For example, the 'assimilability' of a country rock xenolith entrained in a magma depends on the size of that xenolith, viscous flow (Sachs & Stange, 1993), as well as the mineralogical composition and melting temperature of the xenolith. In addition, the hydration and temperature of the entraining magma will also be a factor. It has been demonstrated that high-Mg basaltic magmas can ascend turbulently if they have a sufficiently high flow rate and conduit width (Campbell, 1985; Huppert & Sparks, 1985) delaying the formation of chilled margins and bringing hot magma in direct contact with country rocks for longer periods of time. Huppert and Sparks (1985) proposed that maximum contamination can occur in dykes which are at the minimum width for fully turbulent flow (approximately 3m) and evidence of turbulent flow in a basalt conduit has previously been described on the Isle of Mull (Kille *et al.*, 1986).

The Jurassic mudrocks of the Hebrides Basin will predominantly comprise clay minerals and micas, with variable trace element compositions rich in Al, Si, Fe, Mg and Ti. Early-stage melting of micaceous xenoliths has been shown to occur as an active melt zone at the xenolith rim, depleted in  $\text{Al}_2\text{O}_3$  and enriched in CaO, MgO and  $\text{TiO}_2$  relative to the bulk composition of the xenolith (Shaw, 2009). Trace element mobility (e.g., large ion lithophile elements) will also be affected by the water content of this partial melt. We have tried to relate changes in Skye dyke whole rock geochemistry with  $\delta^{34}\text{S}$  but cannot resolve any correlation between dyke trace element composition and S isotopes. This is possibly because magma compositions were already significantly contaminated by deeper crustal silicic rocks (e.g., Moine and Lewisian basement – see Section 4.4), or due to variations in the original magma compositions (i.e., magma batches) such that trace element variation resulting from later input of Jurassic micaceous material would be masked. In addition, while field relations and hand specimens in our study provide good evidence for mudrock baking, *in situ* anatexis of these crustal rocks is not observed. This is in contrast to millimetre-scale veinlets of

517 anatectic melt a few centimetres from a sill–shale contact (sill is 3 m wide) at Elgol, Skye (Yallup *et*  
518 *al.*, 2013).

519 Sulphur and carbon will be mobilised, even without the need for partial melting *sensu stricto*  
520 (therefore decoupling the trace element geochemistry), and transported as oxidised volatiles  
521 released from the baking of the xenolith and/or sedimentary wall rock. Evidence from mudrocks in  
522 contact with the Cuillin igneous centre on the Isle of Skye suggests that carbon can remain within  
523 these wall-rocks despite severe baking and the high temperatures of the intrusion (Lindgren &  
524 Parnell, 2006). However, this Cuillin study did not investigate the preservation of sulphur. The  
525 thermal effect of the Cuillin Complex was previously recognised as highly localised, using organic  
526 geochemical molecular maturity parameters (Thrasher, 1992). Similarly this localised thermal  
527 alteration has been found to be the case in limestone beds underlying the Trotternish Sills at Staffin  
528 Bay (Lefort *et al.*, 2012). Nevertheless, sediments underlying sills at Duntulm show a more developed  
529 contact metamorphic sequence, including grossular garnet and pyroxene (contact metamorphism)  
530 and low-temperature alteration in microfractures containing clays (Kemp *et al.*, 2005).

531 A doleritic sill at Elgol (southern Skye) that intruded through the Middle Jurassic Cullaidh Shale  
532 formation demonstrates that both sulphur and carbon may be baked out of sediments in this  
533 setting, up to 80 cm from the sill-sediment contact (Yallup *et al.*, 2013). We suggest that a similar  
534 amount of sulphur assimilation took place during the intrusion of the Trotternish Sill Complex (scaled  
535 to the thicker, and presumably long-lived, sill complex). Yallup *et al.* (2013) also demonstrated that  
536  $\delta^{34}\text{S}$  became lighter towards the sediment-sill contact, and suggested that this is due to loss of  $^{34}\text{S}$ -  
537 enriched  $\text{SO}_2$  gas during sediment baking. We cannot demonstrate this feature in the Jurassic  
538 sediments at the base Trotternish sills due to the extremely low concentration of sulphur remaining  
539 in these rocks (almost devoid of S) probably due to substantial baking (and complete loss) of the  
540 sedimentary volatile budget.



On a global scale, the intrusion of sills (as part of large igneous provinces) into thick organic-rich sedimentary basins has been investigated by Svensen and co-workers. For example, hydrothermal vents originating from the base of sills have been identified in the Karoo Basin of South Africa (Svensen *et al.*, 2006, 2007), Siberian Traps (Svensen *et al.*, 2009) and Vøring Basin offshore Norway (Svensen *et al.*, 2004; Planke *et al.*, 2005). These form when large volumes of volatiles (C, S, H<sub>2</sub>O) are baked out of sediments into which magmas have been intruded, and represent significant input of greenhouse gases into the atmosphere at a time coincident with global warming events and/or mass extinctions (e.g., Svensen *et al.*, 2012 and references therein). Most of the aforementioned studies are concerned with the input of C or C-based gases, and have not fully investigated fluxing of S. Nonetheless, in this study we demonstrate the decoupled mobility of S from other trace elements, and highlight the requirement for future investigations into the relative mobilities of C and S (SO<sub>2</sub> is also an important greenhouse gas).

As magma ascends between clay-poor and clay-rich horizons, the amount of water and volatiles released will vary, with volatile-rich shales expected to chemically perpetuate the contamination process. Furthermore the mechanical properties of a shale horizon may actively promote magma penetration. At shallow depths, over-pressured shale units can act as 'ductile horizons', permitting sill formation below the expected level of neutral buoyancy, leading to sill inflation and fracturing of the country rock. This has been documented in the NAIP in the Judd Basin where Palaeogene magmas have intruded through a thick sequence of Jurassic-Palaeocene sediments, forming saucer-shaped sills (Thomson & Schofield, 2008). It is possible that a similar mechanism of intrusion was in operation during formation of the Trotternish Sill Complex on Skye (Fig. 8a). We suggest that this entailed a comparatively 'passive' (i.e., predominantly non-brittle) emplacement mechanism for the magma, such that limited brecciation and entrainment of Jurassic country rock material took place. Where sediment-magma interaction did take place, probably at the chilled base of the sill complex, and in the vicinity of within-sill rafts of Jurassic sediments up to 10m in thickness (Gibson & Jones, 1991) the sediments became so baked, via contact metamorphism, that volatiles such as S and H<sub>2</sub>O

appear to have been entirely expelled. Many of the sills formed as a result of multiple injections, therefore magma flowing through the centre of the sill complex (i.e., from later injections) would have been effectively isolated from contamination effects in ~ horizontal the sill conduit itself (see Fig. 8a).

The large magma volume represented by the sill complex, and sustained magma throughput (at least in comparison to individual basaltic dykes), could have effectively 'diluted' any crustal sulphur, thereby resulting in a limited change in sulphur concentration and/or  $\delta^{34}\text{S}$  signature in the magma body. This is potentially analogous to conduit settings in Noril'sk, where sulphides which initially evolved following S-saturation, became flushed out (Brügmann *et al.*, 1993; Lightfoot & Keays, 2005). Further, Cu/Pd, S-isotope and S/Se evidence from the sill-like intrusions of the Platreef (Bushveld Complex) suggests that S contamination from crustal rocks occurred early and deeper in the plumbing system below the Platreef (McDonald & Holwell, 2007; McDonald *et al.*, 2009; Sharman *et al.*, 2013). These sulphides were transported away from this deeper zone during renewed/continued magma batch injections and ultimately emplaced in the Platreef itself (Ihlenfeld & Keays, 2011). At Trotternish, prior contamination by deeper crustal material during fractionation is demonstrable through other isotope systems (e.g., Sr, Nd and Pb; Gibson, 1990), and we suggest that contamination continued throughout the ascent of the sill complex's parental magmas. However, it is plausible that the change in the emplacement mechanism, due to the change in orientation (i.e., from vertical ascent to horizontal emplacement) or rheology of the country rocks (i.e., brittle vs. non-brittle deformation), would have significant implications for the conduit shape (Schofield *et al.*, 2012) and degree of magma contamination, and, crucially, influenced element mobility during chemical reaction (Fig. 8a).

By contrast, the vertical dykes on Skye show widespread and exceptional degrees of sedimentary sulphur contamination. As previously mentioned, physical brecciation and entrainment of Jurassic mudrocks is observed, and we suggest that the strong crustal chemical 'interaction' of the dykes (as

demonstrated by the correlation between sulphur concentration and  $\delta^{34}\text{S}$ ; Fig. 4b) is directly related to the magma emplacement mechanism (Fig. 8b). These narrow magma conduits, with comparatively limited magma volume, cooled more rapidly than the sills (as shown by their finer crystalline texture), evidently freezing in the local sulphur contamination signature. Dynamic mixing of magmas between the margins and centre of individual dykes has taken place, thereby imparting the marginal contamination  $\delta^{34}\text{S}$  signature to the dyke centre prior to crystallisation, however this process did not completely equilibrate the crustal sulphur input, so that measurable differences in  $\delta^{34}\text{S}$  of up to 1‰ are observed between margins and centres of a 2m wide dyke. A maximum degree of contamination probably occurred within the initial intrusive pulse of a dyke into any one given sedimentary horizon, with later pulses of magma along that conduit and through the dyke becoming progressively shielded from further contamination. Thus the mechanism of contamination in vertical dykes is likely complicated by multiple injections of magma, forming complex dykes (Fig. 8b). However, most of the examples sampled during this study do not display zoning or banding (with the exception of the dyke at Lealt Quarry), and therefore probably only represent a single magma pulse.

<< insert Fig. 8 >>

#### **5.4. Crustal sulphur sources and contamination potential for Hebridean Scotland and the BPIP**

Identifying the crustal contaminants likely to be responsible for inducing S-saturation in ascending magmas is a key factor in pin-pointing when and where immiscible sulphides and orthomagmatic Ni-Cu-PGE mineralization might have occurred. Therefore we have evaluated the S-isotopic signature of various potential S-bearing contaminants on a more regional scale for the BPIP and Isle of Skye.

Aside from the Jurassic sedimentary rocks discussed so far, other upper-crustal sedimentary formations could also be contributors to the sulphur regime. For example, members of the Sleat and Torridon Groups present along the Sleat Peninsula on Skye, and on the Isle of Rum (Fig. 6, Table 1), irrespective of lithology and location, have positive  $\delta^{34}\text{S}$  signatures, ranging +1.4 to +4.7‰. The

Kinloch Formation mudstone had the highest  $\delta^{34}\text{S}$  value of +4.7‰ (Fig. 6). While it is possible that BPIP magmas could be contaminated by Mesoproterozoic sediments, it is very unlikely that this material produced the light  $\delta^{34}\text{S}$  signature seen in the sills and particularly the dykes of Skye. This is in contrast to the  $\delta^{34}\text{S}$  results of certain members of the Stoer Group from the far NW Scottish mainland at Stoer Point, where values less than -30 ‰ are recorded (Parnell *et al.*, 2010). If this material is widely present in the crust below the Isle of Skye, it is possible that the sulphur isotopic signatures of some of the BPIP magma bodies presented here could have been contaminated by this Stoer Group material. However Parnell *et al.* (2010) highlighted the patchy nature of this light S-isotope signature, with bacterial sulphate reduction constrained within small continental water bodies, the relicts of which are laterally discontinuous along strike. More directly, there is no surface exposure of the Stoer Group extending as far south as the Isle of Skye – only the equivalent Sleat Group is observed in this BPIP area, and as discussed above, analysis of this material indicates that its S isotope signature is significantly heavier. Therefore the combination of the extremely heterogeneous sulphur isotope signature, and unconstrained subterranean extent of the Stoer Group, and other Torridonian sediments, makes this an unlikely candidate to explain the uniformly light  $\delta^{34}\text{S}$  of the dykes and sills on Skye.

There is ample evidence that deeper crustal contamination via assimilation fractional crystallization (AFC) and assimilation during turbulent ascent (ATA), took place across the BPIP. This includes large deep staging chamber settings, or in narrower meter-scale magma conduits. Both Lewisian (granulite and amphibolite-facies) and Moinian contaminants have been successfully shown to explain the Sr, Nd, and Pb isotopic heterogeneities observed in BPIP magmas (e.g., Gibson, 1990; Kerr, 1995; Preston *et al.*, 1998). In particular, Gibson (1990) demonstrated that the Trotternish Sill Complex underwent up to ~20% mid- or lower-crustal contamination, prior to magma injection and emplacement. Thompson (1982) and Gibson (1990) use La/Nb ratios to constrain assimilation of Lewisian rocks by Palaeogene magmas, now preserved as dykes, sills and lavas. There is no correlation between La/Nb ratio and  $\delta^{34}\text{S}$  for dykes included in this study (refer to Supplementary

Material). There is a very weak and inconclusive correlation between La/Nb ratio vs.  $\delta^{34}\text{S}$  for sills ( $r^2 = 0.31$ ). Lewisian gneisses have variable, but low sulphur concentrations and  $\delta^{34}\text{S}$  ranging -1.4 to +1.2‰ (this study) and -1.4 to +5.5‰ on the NW Scottish mainland (Lowry *et al.*, 2005). Torridonian sediments measured in this study always have  $\delta^{34}\text{S} > 0$ ‰. Moine metapelites also have low or very low concentrations of sulphur, and where measurable have  $\delta^{34}\text{S} = +2.5$ ‰ (this study) and +3.4 to +4.6‰ in some psammites (Lowry, 1991). Accordingly, Lowry *et al.*, (2005) found that each crustal terrane across Scotland could be characterised by its dominant crustal units, reflected in the range of  $\delta^{34}\text{S}$  for that region. In the Northern Highland Terrane (which includes Skyes) complexities in the terrane-scale  $\delta^{34}\text{S}$  were suggested as reflecting the thick North Atlantic Craton (i.e., Lewisian and Palaeoproterozoic metasediments of Loch Maree) underlying the upper crustal sedimentary cover.

Our study shows that both the Moine and Lewisian deeper crustal materials are unrealistic sources for the consistent and characteristically light sulphur isotopic signature of the Skye dykes. Therefore, we suggest that while deep crustal contamination of BPIP magmas has taken place, the dominant  $\delta^{34}\text{S}$  contamination signature observed in these magmas is the result of specific and localised upper-crustal contamination of readily-fusible, organic-rich Jurassic shales and mudrocks. This has taken place in smaller vertical magma conduits, or where the mudrocks were in direct contact with BPIP magmas, allowing for pervasive alteration, mobilisation of volatiles and in some cases physical and chemical assimilation of these country rocks, modelled by a simple binary mixing scenario.

## **5.5. Implications for Ni-Cu-PGE orthomagmatic sulphide mineralization**

Whilst not the sole forcing factor in the occurrence of S-saturation, significant literature points to the common association of crustal contamination with the development of orthomagmatic sulphide mineralization (e.g., Noril'sk-Talnakh Region (Ripley *et al.*, 2003; Ripley & Li, 2013); Duluth (Arcuri *et al.*, 1998); Voisey's Bay (Ripley *et al.*, 1999); Kambalda (Leshner & Burnham, 2001); and others (see Naldrett 2004, 2011 and references therein). A scenario where crustal sulphur is available for magma contamination is therefore often an important factor in Ni-Cu-PGE exploration. A recent

study of lavas by Hughes *et al.* (under review) has suggested that Scottish BPIP is one of the most fertile regions of the NAIP for Ni-Cu-PGE mineralisation, in part due to the widespread opportunities for shallow crustal contamination by S-rich sediments.

Interpreting sulphide metal tenors and whole-rock chalcophile element abundances of magmas in relation to their degree of crustal sulphur contamination (monitored here by  $\delta^{34}\text{S}$ ) can be complicated by the formation of multiple generations of sulphide liquids (i.e., deeper in the magmatic plumbing system; e.g., Holwell *et al.*, 2007) and the effects of prolonged interaction of sulphides with fresh silicate magma(s) (Campbell & Naldrett, 1979). The ultramafic sills have a low Cu/Pd ratio (13300 to 46200) in comparison to most of the basaltic Robustan dykes (5590 and 167200), however this ratio is still elevated above that of primitive mantle (c. 7000-8000 based on pyrolite; McDonough & Sun, 1995), suggesting that sulphide saturation had probably already taken place prior to emplacement of the sills. The highly variable Cu/Pd ratio of the Robustan dykes is likely also recording one or more S-saturation events which occurred prior to dyke emplacement. However because the dykes are demonstrably assimilating local crustal sulphur at the current erosion level, we can further inspect the response of the remaining low-abundance chalcophile elements to this secondary S-saturation event.

Broadly, dyke samples with the lightest crustal  $\delta^{34}\text{S}$  signatures have the lowest Pd concentration (Fig. 5a) and highest Cu/Pd ratio (Fig. 5c). Pt, Pd and Au concentrations show the strongest response to localised crustal S contamination, and variations in Cu appear to be weaker (i.e., less variable concentrations) in this secondary S-saturation scenario. This causes a correspondingly 'delayed' spike in Cu/Pd ratio. In PGE mineralised settings (e.g., the Bushveld Complex) this feature is well documented for S-saturation in PGE reefs (Maier, 2005 and references therein) as the partition coefficient of Pd into sulphide liquid is several orders of magnitude greater than that for Cu (Mungall *et al.*, 2005; Mungall & Brenan, 2014). However in a setting where first-stage S-saturation has already occurred deeper in the system, the concentration of chalcophile elements (particularly Pd-

group PGE) would be much lower in the remaining silicate magma that continued its ascent to the surface. Therefore the Cu/Pd ratio of that residual silicate magma would be much higher and more variable than that of a magma which had only undergone one S-saturation event (as seen in the Trotternish Sills). From this secondary 'starting point' Cu/Pd ratio, a second-stage localised S-saturation event would lead to further fractionation of Pd from Cu (particularly for systems with low R-factors; the ratio of sulphide liquid to silicate magma), raising Cu/Pd ratio to even higher values (up to 167,000 in sample SK131). Assuming sulphide liquids from the initial S-saturation event had not been entrained during continued magma ascent, the extreme variability in Cu/Pd ratio caused by this first S-saturation (deeper) would lead to even greater erraticism in this parameter during the formation of later sulphide liquids (shallower). Thus, in the absence of entrained sulphide liquids, the detailed interpretation of chalcophile element ratios at/after secondary S-saturation events would be impractical.

The cause for this first-stage S-saturation event remains speculative – given the silicic basement underlying this region, this could have been due to the addition of SiO<sub>2</sub> to the magma (as well as fractional crystallisation during magma ascent) such that S concentration at sulphide-saturation (SCSS) was lowered. Alternatively this could have been triggered by addition of S deeper in the crust, but during this study we have shown that  $\delta^{34}\text{S}$  of Moine, Torridonian and Lewisian rocks is within magmatic variation ( $0 \pm 4\text{‰}$ ) and therefore would not be detected by this method. However, we have also determined that S abundance in these lithologies is typically very low, and we question the likelihood of these rocks in contributing enough S during deep crustal contamination to induce S-saturation.

Ultimately the effects of multiple S-saturation events might be further investigated by analysis of the S/Se ratio of sulphide minerals (e.g., Ihlenfeld & Keays, 2011). In addition, the earlier S-saturation of magmas would likely preclude significant orthomagmatic Ni-Cu-PGE mineralization in higher portions of a magmatic province. However, by identifying the physical and structural factors

controlling the ability of an ascending magma to assimilate crustal sulphur in a conduit, we can ascertain the locations within a magmatic plumbing system (deep or shallow) where S-saturation is likely to have taken place, leading to mineralization.

Finally, the small ( $\pm 1.4\%$ ) and non-systematic variation observed between  $\delta^{34}\text{S}$  of sulphide minerals (in this case, pyrite) compared to whole-rock values is acceptable for use in identifying the occurrence of contamination of magmas by crustally-derived sulphur. The observed maximum procedural-induced isotopic shift is very small in comparison to the isotopic shift caused by crustal contamination and the natural  $\delta^{34}\text{S}$  of the country rock samples. However this is dependent on the crustal sulphur source having a characteristic  $\delta^{34}\text{S}$  signature (either light or heavy), and being statistically different from the typical 'mantle' signature. Therefore the whole-rock CRS method of sample preparation for  $\delta^{34}\text{S}$  analysis (as used in this study) is suitable for identifying areas of potential sulphur saturation in mantle-derived magmas contaminated by crustal sulphur. This contributes to a rapid and flexible exploration tool for orthomagmatic Ni-Cu-PGE sulphide deposits, applicable even to samples with non-visible sulphide mineralization, as it identifies crustal sulphur contamination of whole-rock magmatic samples, assuming that there is a significant difference between the sedimentary and mantle  $\delta^{34}\text{S}$  composition. This method offers the opportunity to vector into areas of increased crustal S contamination, even in relatively S-poor rocks.



## 6. Conclusions

1. The  $\delta^{34}\text{S}$  range for the Palaeogene alkali picritic Trotternish Sill Complex (+0.1 to -4.9‰; mean =  $-2.3 \pm 1.5\text{‰}$ ) reflects the dominance of mantle-derived sulphur, consistent with that found in other Icelandic mantle plume-derived magmas.
2. In contrast, the observed  $\delta^{34}\text{S}$  range for the Palaeogene basaltic Robustan dykes is -2.3 to -30.7‰. Sulphur isotope evidence for contamination is present throughout the full widths of these dykes: margins and centres alike.
3. There appears to be a fundamental geological control on the degree of crustal contamination of magma bodies, depending of the mechanism (orientation and energy) by which that magma intruded. In spite of similar country rocks characterised by light  $\delta^{34}\text{S}$  ( $> -33.8\text{‰}$ ), there is a distinct difference in the S contamination pattern between a flat-lying concordant and thicker magma conduit (as represented by the 10-100m-scale Trotternish Sill Complex,  $\delta^{34}\text{S}$  from -4.9 to +0.1‰ with one outlier of -10.8‰), and a vertically intruded discordant and narrow magma conduit (meter-scale basaltic Robustan dykes,  $\delta^{34}\text{S}$  from -2.3 to -30.7‰).
4. Turbulent flow within narrow magma conduits emplaced discordantly to sediments maximises contamination potential, particularly of volatile and highly mobile elements (such as S) in a high surface-to-volume scenario. Whereas passively emplaced, wide conduits emplaced concordantly to the sediments undergo comparatively little crustal sulphur contamination. This mechanical control may act in addition to other known controls on contamination such as the temperature and flux rate of magma in a conduit system.
5. Despite the absence of sulphide minerals, a S-saturation event prior to dyke emplacement may be identified using Cu/Pd ratio. Given the high concentration of S in these dykes, and their strong  $\delta^{34}\text{S}$  crustal contamination signature, S-saturation causing this extreme variability in Cu/Pd ratio must have been imparted before dyke emplacement and therefore at a deeper

crustal level. This suggests that Ni-Cu-PGE mineralisation may exist below current exposure levels. However the trigger for this previous S-saturation remains unresolved.

6. Where sulphide minerals are either too rare or too small to separate, use of whole-rock sulphur extraction to analyse  $\delta^{34}\text{S}$  in samples can reveal S contamination. We suggest that this technique offers a suitable and rapid method that can be used as a vectoring tool for exploration of orthomagmatic Ni-Cu-PGE mineralization.

767    *Acknowledgements*

768    *Sulphur isotope analysis was undertaken at the Scottish Universities Environment Research Centre*  
769    *(SUERC) and funded by a NERC Isotope Geosciences Facilities Steering Committee grant (IP-1356-*  
770    *1112). HSRH would like to acknowledge the financial support of the Natural Environment Research*  
771    *Council (NERC) for funding this work (studentship NE/J50029X/1) and open access publication. AJB is*  
772    *funded by NERC funding of the Isotope Community Support Facility at SUERC. The manuscript*  
773    *benefitted from discussions with Ben Manton, Geoff Steed and Andrew Kerr. Sally Gibson and*  
774    *Bernard Bingen are thanked for their thorough and constructive reviews.*

775

776 **Figure captions**

777 **Figure 1** – (a) Location and simplified geological map of part of the British Palaeogene Igneous  
778 Complex (BPIP) – the geology of the Isle of Skye, Rum and the Small Isles. Two black boxes highlight  
779 close-up geological maps (see Supplementary Material B). Light grey background does not delineate  
780 specific geology, but we highlight that the Lewisian gneisses underlie this entire region (north of the  
781 Great Glen Fault). (b) Hebrides Basin sediments area surrounding the Isle of Skye and the Small Isles.  
782 Adapted from Fyfe *et al.*, (1993).

783 **Figure 2** – Strathaird Peninsula (southern Skye). Line of cross-section displays position of the dyke  
784 samples as projected parallel to the strike of the sediment bedding planes, with the exception of  
785 sample SK40, which has been projected onto the cross-section along the strike of the dyke itself.  
786 Dykes drawn assuming vertical dip. Sediments dip approximately 10° dip NNW below the sediment-  
787 lava contact at Scaladal Burn (note cross-section shows 2 x vertical exaggeration). Extent of dyke  
788 structure under the current surface level is unknown – cross-section projects dykes for display  
789 purposes only.

790 **Figure 3** (*colour online*) – Annotated photographs of field relations for the Trotternish Sills and cross-  
791 cutting dykes on the Trotternish Peninsula. (a) Lealt Quarry (looking West) – Horizontal Trotternish  
792 Sills cross-cut by a later, banded basalt dyke. (b) Close-up of Northern margin of basalt dyke in Lealt  
793 Quarry showing both picrite (white lines) and mudrock (black lines) xenoliths in a fluid-rich coarser  
794 section of the dyke approximately 10cm from the chilled margin. Some mudrock xenoliths have  
795 begun to disintegrate and ‘fray’ at the edges, becoming assimilated or with ribbon-like fluid-rich  
796 trails extending into the basalt. (c) Faint banding in the central portions of the dyke. Some ‘bands’  
797 have elongate mudrock xenolith trails. (d) Close-up of the Southern margin of the basalt dyke at  
798 Lealt Quarry showing trails of white zeolites close to the chilled margin (annotated by black dashed

circles). Baked mudrock xenolith with white coloured fluid-rich stringers extending into basalt shown at top of the image. Basalt dyke contact with picrite sill is annotated by solid white line, and c. 5mm wide basalt chilled margin by dashed white line. (e) Skudiburgh, looking North, with vertical basalt dyke cross-cutting the horizontally banded Trotternish Sills. No offsets of dyke or sills, despite the angle of the photograph. Base of the sill package delineated by black solid line, which overlies a poorly exposed area of baked mudrocks (best observed in the area delineated by dashed black lines).

**Figure 4** – Sulphur isotope ( $\delta^{34}\text{S}$ ) results for Isle of Skye sills and dykes (a) All sills and dykes. (b) Correlation between whole-rock S concentration and  $\delta^{34}\text{S}$  for Robustan dykes (line of best fit is a logarithmic fit as shown, but a linear fit also produces  $r^2$  value  $> 0.95$ ). See main text in Section 4.2 for further details.

**Figure 5** – Sulphur isotope ( $\delta^{34}\text{S}$ ) results (grey histograms) and whole-rock PGE and Cu concentrations and ratios (black lines with circles) for the basaltic Robustan dykes, aligned according to a NW-SE transect, as displayed in the cross-section of Figure 2. (a) Pd (ppb) and  $\delta^{34}\text{S}$ , (b) Cu (ppm) and  $\delta^{34}\text{S}$ , (c) Cu/Pd  $\times 1000$  ratio and  $\delta^{34}\text{S}$ , and (d) Pt/Pd ratio and  $\delta^{34}\text{S}$ . The light grey shaded areas in (c) delineates the range of Cu/Pd ratios measured in samples from the Trotternish Sill Complex and dark grey delineates mantle ranges (according to McDonough & Sun, 1995).

**Figure 6** – Sulphur isotope ( $\delta^{34}\text{S}$ ) results for Jurassic and Torridonian (Mesoproterozoic) sediment samples from the Hebrides Basin area, Isle of Skye, Isle of Rum, and Ardnamurchan.

**Figure 7** – (a) Simple binary mixing model between a mantle melt (starting  $\delta^{34}\text{S} = 0.0\text{‰}$ , 250ppm S) end member, and a contaminating end member of either Staffin Bay Formation sandstone, sample SK53 ( $\delta^{34}\text{S} = -33.8\text{‰}$ ,  $< 180\text{ppm S}$ ) or Staffin Shale Formation shale unit, sample SK50 ( $\delta^{34}\text{S} = -32.6\text{‰}$ , 1130 ppm S). Overlain on the plot are basalt dyke samples SK127, SK128, SK129 and SK131, with estimates of 'f' (mass fraction of S from the contaminating end member) for each sample.

**Figure 8** – (a) Passive intrusion of magmas forming sills – while the ~ vertical oriented feeder zone(s) are likely to actively assimilate and become contaminated by wall rocks during magma ascent, once the magma reaches a ductile horizon or zone of neutral buoyancy (spreading out horizontally) it is emplaced in a ‘passive’ environment of inflation. In this ‘passive’ setting, little physical attrition of wall rocks will occur so that little/no crustal S-isotope signature is imparted. (b) Active intrusion of magmas forming dykes – the ~ vertical and high-energy intrusion of magmas into upper crustal levels forming dykes (e.g., at Lealt Quarry or Robustan) causes physical attrition/brecciation of wall rocks. This higher energy (or ‘active’) or mechanism of emplacement leads to the entrainment of xenoliths (via wall rock attrition) and chemically leaches wall rocks of volatiles (S), imparting a crustal S-isotopic signature. In both cases (a) and (b), the contamination signature is inferred to be a local effect (magmas have transported the signature on a maximum scale of 100’s meters). See main text (Section 5.3.1) for further details.

836

837 **Table captions**

838 **Table 1** – Summary of sulphur isotopic compositions ( $\delta^{34}\text{S}$ ) measured by conventional methodology  
839 (following whole-rock sulphur extraction; indicated as 'wr') and laser combustion methodology  
840 (indicated as 'Laser'). Whole-rock S concentration (in wt. %) is also listed. In instances where a  
841 powdered sample was subjected to the whole-rock sulphur extraction (CRS) method, but no  
842 precipitate was yielded or the precipitate was too small to facilitate conventional analysis, 'no  
843 precipitate' is annotated in Table 1. (\*)Indicates that the S concentration of this sample was too high  
844 to be determined (based on the calibrated set-up of LECO) and thus the estimated S concentration is  
845 listed in Table 1. Note that samples with S concentration below detection limit are indicated by <  
846 0.02 (detection limit). Full mineral-specific and duplicate sample details are available in the  
847 Supplementary Material.

848

849     References:

850

851     AARNES, I., SVENSEN, H., CONNOLLOY, J.A.D., PODLADCHIKOV, Y.Y. 2010. How contact metamorphism can  
852             trigger global climate changes: Modeling gas generation around igneous sills in sedimentary  
853             basins. *Geochimica et Cosmochimica Acta*, **74**, 7179-7195.

854     AARNES, I., SVENSEN, H., POLTEAU, S., PLANKE, S. 2011. Contact metamorphic devolatilization of shales in  
855             the Karoo Basin, South Africa, and the effects of multiple sill intrusions. *Chemical Geology*,  
856             **281**, 181-194.

857     ALT, J., SHANKS, W. & JACKSON, M. 1993. Cycling of sulphur in subduction zones: the geochemistry of  
858             sulphur in the Mariana Island Arc and back-arc trough. *Earth and Planetary Science Letters*,  
859             **119**, 477-494.

860     ANDREWS, J. E., HAMILTON, P. J. & FALICK, A. E. 1987. The geochemistry of early diagenetic dolostones  
861             from a low-salinity Jurassic lagoon. *Journal of the Geological Society, London*, **144**, 687-698.

862     ARCURI, T., RIPLEY, E. M. & HAUCK, S. A. 1998. Sulphur and oxygen isotope studies of the interaction  
863             between pelitic xenoliths and basaltic magma at the Babbitt and Serpentine Cu-Ni deposits,  
864             Duluth Complex, Minnesota. *Economic Geology*, **93**, 1063-1075.

865     BELL, B.R. & WILLIAMSON, I.T. 2002. Tertiary volcanism. In *The Geology of Scotland*, 4th edition (ed.  
866             N.H.TREWIN), 317-407. The Geological Society

867     BECKINSALE, R. D., PANKHURST, R. J., SKELHORN, R. R. & WALSH, J. N. 1978. Geochemistry and petrogenesis  
868             of the Early Tertiary lava pile of the Isle of Mull, Scotland. *Contributions to Mineralogy and*  
869             *Petrology*, **66**, 415-427.

870     BRÜGMANN, G. E., NALDRETT, A. J., ASIF, M., LIGHTFOOT, P., *et al.* 1993. Siderophile and chalcophile  
871             metals as tracers of the evolution of the Siberian Trap in the Noril'sk region, Russia.  
872             *Geochimica et Cosmochimica Acta*, **57**, 2001-2018.

873     CAMPBELL, I. H. 1985. The difference between oceanic and continental tholeiites: a fluid dynamic  
874             explanation. *Contributions to Mineralogy and Petrology*, **91**, 37-43.



875 CAMPBELL, I. H. & NALDRETT, A. J. 1979. The influence of silicate:sulphide ratios on the geochemistry of  
876 magmatic sulphides. *Economic Geology*, **74**, 1503-1506.

877 CANFIELD, D., RAISWELL, R., WESTRICH, J., REAVES, C., *et al.* 1986. The use of chromium reduction in the  
878 analysis of reduced inorganic sulphur in sediments and shales. *Chemical Geology*, **54**, 149-  
879 155.

880 CANFIELD, D.E. & TESKE, A. 1996. Late Proterozoic rise in atmospheric oxygen concentration inferred  
881 from phylogenetic and sulphur-isotope studies. *Nature*, **382**, 127-132.

882 COLEMAN, M. L. & MOORE, M. P. 1978. Direct reduction of sulphates to sulphur dioxide for isotopic  
883 analysis. *Analytical Chemistry*, **28**, 199-260.

884 DICKIN, A. P. 1981. Isotope geochemistry of Tertiary igneous rocks from the Isle of Skye. *Journal of*  
885 *Petrology*, **22**, 155-190.

886 DICKIN, A. P., JONES, N. W., THIRLWALL, M. F. & THOMPSON, R. N. 1987. A Ce/Nd isotope study of crustal  
887 contamination processes affecting Palaeocene magmas in Skye, Northwest Scotland.  
888 *Contributions to Mineralogy and Petrology*, **96**, 455-464.

889 EMELEUS, C. H. & BELL, B. R. 2005. *British Regional Geology: The Palaeogene volcanic districts of*  
890 *Scotland*, Nottingham, British Geological Survey.

891 FISHER, I. ST J, & HUDSON, J. D. 1987. Pyrite formation in Jurassic shales of contrasting biofacies.  
892 *Geological Society Special Publication*, **26**, 69-78.

893 GIBB, F.G.F. & GIBSON, S.A. 1989. The Little Minch Sill Complex. *Scottish Journal of Geology*, **25**, 367-  
894 370.

895 GIBSON, S. A. 1990. The geochemistry of the Trotternish sills, Isle of Skye: crustal contamination in the  
896 British Tertiary Volcanic Province. *Journal of the Geological Society, London*, **147**, 1071-1081.

897 GIBSON, S. A. & JONES, A. P. 1991. Igneous stratigraphy and internal structure of the Little Minch Sill  
898 Complex, Trotternish Peninsula, northern Skye, Scotland. *Geological Magazine*, **128**, 51-66.

899 HALL, G. E. M., PELCHAT, J.-C. & LOOP, J. 1988. Separation and recovery of various sulphur species in  
900 sedimentary rocks for stable sulphur isotopic determination. *Chemical Geology*, **67**, 35-45.

901 HARKER, A. 1904. The Tertiary Igneous Rocks of Skye. *Memoir of the Geological Survey of Great*  
902 *Britain*, HMSO, Edinburgh.

903 HESSELBO, S. P. & COE, A. L. 2000. Jurassic sequences of the Hebrides Basin, Isle of Skye, Scotland. *In:*  
904 *Field Trip Guidebook*. (eds. GRAHAM, J. R. & RYAN, A.), pp. 41-58. Dublin: International  
905 Association of Sedimentologists.

906 HOLWELL, D.A., BOYCE, A.J. & McDONALD, I. 2007. Sulphur isotope variations within the Platreef Ni-Cu-  
907 PGE deposit: Genetic implications for the origin of sulphide mineralization. *Economic*  
908 *Geology*, **102**, 1091-1110.

909 HUBER, H., KOEBERL, C., McDONALD, I. & REIMOND, W. U. 2000. Use of  $\gamma$ - $\gamma$  coincidence spectrometry in  
910 the geochemical study of diamictites from South Africa. *Journal of Radioanalytical and*  
911 *Nuclear Chemistry*, **244**, 603-607.

912 HUDSON, J. D., COLEMAN, M. L., BARREIRO, B. A. & HOLLINGWORTH, N. T. J. 2001. Septarian concretions  
913 from the Oxford Clay (Jurassic, England, UK): involvement of original marine and multiple  
914 external pore fluids. *Sedimentology*, **48**, 507-531.

915 HUGHES, H.S.R., McDONALD, I., KERR, A.C. (under review). Platinum group element signatures in the  
916 North Atlantic Igneous Province: Implications for mantle controls on metal budgets during  
917 continental breakup. *Lithos*.

918 HUPPERT, H. E. & SPARKS, S. J. 1985. Cooling and contamination of mafic and ultramafic magmas  
919 during ascent through continental crust. *Earth and Planetary Science Letters*, **74**, 371-386.

920 IHLENFELD, C. & KEAYS, R. R. 2011. Crustal contamination and PGE mineralization in the Platreef,  
921 Bushveld Complex, South Africa: evidence for multiple contamination events and transport  
922 of magmatic sulphides. *Mineralium Deposita*, **46**, 813-832.

923 JUGO, P. J. 2004. An Experimental Study of the Sulphur Content in Basaltic Melts Saturated with  
924 Immiscible Sulphide or Sulphate Liquids at 1300 C and 1{middle dot}0 GPa. *Journal of*  
925 *Petrology*, **46**, 783-798.

926 KEMP, S. J., ROCHELLE, C. A. & MERRIMAN, R. J. 2005. Back-reacted saponite in Jurassic mudstones and  
 927 limestones intruded by a Tertiary sill, Isle of Skye. *Clay Minerals*, **40**, 263-282.

928 KENT, R. W., THOMSON, B. A., SKELHORN, R. R., KERR, A. C., *et al.* 1998. Emplacement of Hebridean  
 929 Tertiary flood basalts: evidence from an inflated pahoehoe lava flow on Mull, Scotland.  
 930 *Journal of the Geological Society, London*, **155**, 599-607.

931 KERR, A. C. 1995. The geochemistry of the Mull-Morvern lava succession, NW Scotland: an  
 932 assessment of mantle sources during plume-related volcanism. *Chemical Geology*, **122**, 43-  
 933 58.

934 KERR, A. C. 1997. The geochemistry and significance of plugs intruding the Tertiary Mull-Morvern lava  
 935 succession, western Scotland. *Scottish Journal of Geology*, **33**, 157-167.

936 KILLE, I. C., THOMPSON, R. N., MORRISON, M. A. & THOMPSON, R. F. 1986. Field evidence for turbulence  
 937 during flow of basalt magma through conduits from southwest Mull. *Geological Magazine*,  
 938 **123**, 693-697.

939 KINNAIRD, T. C., PRAVE, A. R., KIRKLAND, C. L., HORSTWOOD, M., *et al.* 2007. The late Mesoproterozoic-  
 940 early Neoproterozoic tectonostratigraphic evolution of NW Scotland: the Torridonian  
 941 revisited. *Journal of the Geological Society*, **164**, 541-551.

942 KUSAKABE, M., MAYEDA, S. & NAKAMURA, E. 1990. S, O and Sr isotope systematics of active vent  
 943 materials from the Mariana Back Arc Basin spreading axis at 18 N. *Earth and Planetary  
 944 Science Letters*, **100**, 275-282.

945 LABIDI, J., CARTIGNY, P., BIRCK, J. L., ASSAYAG, N., *et al.* 2012. Determination of multiple sulphur isotopes  
 946 in glasses: A reappraisal of the MORB  $\delta^{34}\text{S}$ . *Chemical Geology*, **334**, 189-198.

947 LEFORT, A., HAUTEVELLE, Y., LATHUILIERE, B. & HUAULT, V. 2012. Molecular organic geochemistry of a  
 948 proposed stratotype for the Oxfordian/Kimmeridgian boundary (Isle of Skye, Scotland).  
 949 *Geological Magazine*, **149**, 857-874.

950 LESHER, C. E. & BURNHAM, O. M. 2001. Multicomponent elemental and isotopic mixing in Ni-Cu-(PGE)  
 951 ores at Kambalda, Western Australia. *The Canadian Mineralogist*, **39**, 421-446.

952 LIGHTFOOT, P. & KEAYS, R. R. 2005. Siderophile and chalcophile metal variations in flood basalts from  
 953 the Siberian Trap, Noril'sk Region: Implications for the origin of the Ni-Cu-PGE sulphide ores.  
 954 *Economic Geology*, **100**, 439-462.

955 LINDGREN, P. & PARNELL, J. 2006. Rapid heating of carbonaceous matter by igneous intrusions in  
 956 carbon-rich shale, Isle of Skye, Scotland: an analogue for heating of carbon in impact  
 957 craters? *International Journal of Astrobiology*, **5**, 343-351.

958 LOWRY, D., 1991. *The genesis of Late Claedonian granitoid-related mineralization in Northern Britain*.  
 959 Unpublished PhD thesis, University of St Andrews.

960 LOWRY, D., BOYCE, A. J., FALICK, A. E. & STEPHENS, W. E. 1995. Genesis of porphyry and plutonic  
 961 mineralisation systems in metaluminous granitoids of the Grampian Terrane, Scotland.  
 962 *Transactions of the Royal Society of Edinburgh: Earth Sciences*, **85**, 221-237.

963 LOWRY, D., BOYCE, A.J., FALICK, A.E., STEPHENS, W.E. & GRASSINEAU, N.V. 2005. Terrane and  
 964 basement discrimination in northern Britain using S isotopes and mineralogy of ore deposits.  
 965 *In: MCDONALD, I., BOYCE, A.J., BUTLER, I.B., HERRINGTON, R.J. & POLYA, D.A. (eds) Deposits*  
 966 *and Earth Evolution. Geological Society, London, Special Publications*, **248**, 133-151.

967 MAIER, W. D. 2005. Platinum-group element (PGE) deposits and occurrences: Mineralization styles,  
 968 genetic concepts, and exploration criteria. *Journal of African Earth Sciences*, **41**, 165-191.

969 MAYER, B. & KROUSE, H. 2004. Procedures for sulphur isotope abundance studies. *In: Handbook of*  
 970 *Stable Isotope Analytical Techniques*. pp. 538-596. Elsevier.

971 MCDONALD, I. & HOLWELL, D. A. 2007. Distribution of platinum-group elements in the Platreef at  
 972 Overysel, northern Bushveld Complex: a combined PGM and LA-ICP-MS study. *Contributions*  
 973 *to Mineralogy and Petrology*, **154**, 171-190.

974 MCDONALD, I., HOLWELL, D. A. & Wesley, B. 2009. Assessing the potential involvement of an early  
 975 magma staging chamber in the generation of the Platreef Ni-Cu-PGE deposit in the  
 976 northern limb of the Bushveld Complex: a pilot study of the Lower Zone Complex at

977 Zwartfontein . *Applied Earth Science (Transactions Institute of Mining & Metallurgy B)* **118**,  
978 5-20.

979 McDONALD, I. & VILJOEN, K. S. 2006. Platinum-group element geochemistry of mantle eclogites: a  
980 reconnaissance study of xenoliths from the Orapa kimberlite, Botswana. *Applied Earth*  
981 *Science*, **115**, 81-93.

982 McDONOUGH, W. F. & SUN, S. 1995a. The Composition of the Earth. *Chemical Geology*, **120**, 223-253.

983 MOORBATH, S. & THOMPSON, R. N. 1980. Strontium isotope geochemistry and petrogenesis of the Early  
984 Tertiary lava pile of the Isle of Skye, Scotland, and other basic rocks of the British Tertiary  
985 Province: an example of magma-crust interaction. *Journal of Petrology*, **21**, 295-321.

986 MORTON, N. & HUDSON, J. D. 1995. Field guide to the Jurassic of the Isles of Raasay and Skye, Inner  
987 Hebrides, NW Scotland. *In: Field geology of the British Jurassic*. (eds. TAYLOR, P. D.). The  
988 Geological Society, London.

989 MUNGALL, J., ANDREWS, D., CABRI, L., SYLVESTER, P., *et al.* 2005. Partitioning of Cu, Ni, Au, and platinum-  
990 group elements between monosulphide solid solution and sulphide melt under controlled  
991 oxygen and sulphur fugacities. *Geochimica et Cosmochimica Acta*, **69**, 4349-4360.

992 MUNGALL, J. E. & BRENNAN, J. M. 2014. Partitioning of platinum-group elements and Au between  
993 sulphide liquid and basalt and the origins of mantle-crust fractionation of the chalcophile  
994 elements. *Geochimica et Cosmochimica Acta*, **125**, 265-289.

995 NALDRETT, A. J. 2004. *Magmatic sulphide deposits: geology, geochemistry and exploration*, Berlin,  
996 Springer.

997 NALDRETT, A. J. 2011. Fundamentals of Magmatic Sulphide Deposits. *In: Magmatic Ni-Cu and PGE*  
998 *deposits: geology, geochemistry, and genesis*. (eds. LI, C. & RIPLEY, E. M.), pp. 1-51. Society of  
999 Economic Geologists, Reviews in Economic Geology volume 17.

1000 NEWTON, R. J., BOTTRELL, S. H., DEAN, S. P., HATFIELD, D., *et al.* 1995. An evaluation of the use of the  
1001 chromous chloride reduction method for isotopic analyses of pyrite in rocks and sediment.  
1002 *Chemical Geology*, **125**, 317-320.

1003 NIELSEN, J. K. & HANKEN, N.-M. 2002. Description of the chromium reduction method for extraction of  
 1004 pyrite sulphur. University of Tromsø.

1005 OHMOTO, H., & GOLDBERGER, M. B., 1997, Sulphur and carbon isotopes. *In: Geochemistry of*  
 1006 *hydrothermal ore deposits*. (ed. Barnes, H. L.), 3rd edition: New York, Wiley, p. 517–611.

1007 OHMOTO, H. & RYE, R. O. 1979. Isotope of sulphur and carbon, In: *Geochemistry of Hydrothermal*  
 1008 *deposits*. (ed. Barnes, H. L.), John Wiley & Sons, 509-567.

1009 OXBURGH, E. R., MCRAE, T. & O'HARA, M. J. 1984. Physical Constraints on Magma Contamination in the  
 1010 Continental Crust: An Example, the Adamello Complex [and Discussion]. *Philosophical*  
 1011 *Transactions of the Royal Society A: Mathematical, Physical and Engineering Sciences*, **310**,  
 1012 457-472.

1013 PALACZ, Z. 1985. Sr-Nd-Pb isotopic evidence of crustal contamination in the Rhum intrusion. *Earth*  
 1014 *and Planetary Science Letters*, **74**, 35-44.

1015 PARNELL, J., BOYCE, A. J., MARK, D., BOWDEN, S., *et al.* 2010. Early oxygenation of the terrestrial  
 1016 environment during the Mesoproterozoic. *Nature*, **468**, 290-293.

1017 PARNELL, J., HOLE, M., BOYCE, A. J., SPINKS, S., *et al.* 2012. Heavy metal, sex and granites: Crustal  
 1018 differentiation and bioavailability in the mid-Proterozoic. *Geology*, **40**, 751-754.

1019 PENNISTON-DORLAND, S. C., WING, B. A., NEX, P. A. M., KINNAIRD, J. A., *et al.* 2008. Multiple sulphur  
 1020 isotopes reveal a magmatic origin for the Platreef platinum group element deposit, Bushveld  
 1021 Complex, South Africa. *Geology*, **36**, 979.

1022 PLANKE, S., RASMUSSEN, T., REY, S.S., MYKLEBUST, R. 2005. Seismic characteristics and distribution of  
 1023 volcanic intrusions and hydrothermal vent complexes in the Vøring and Møre basins. In:  
 1024 DORE, T., VINING, B. (Eds.), *Petroleum Geology: North-West Europe and Global Perspectives*,  
 1025 Geological Society Publishing House, London.

1026 PLATTEN, I. M. 2000. Incremental dilation of magma filled fractures: evidence from dykes on the Isle  
 1027 of Skye, Scotland. *Journal of Structural Geology*, **22**, 1153-1164.

1028 PRESTON, R. J., BELL, B. R. & ROGERS, G. 1998. The Loch Scridain sill complex, Isle of Mull, Scotland:  
 1029 fractional crystallization, assimilation, magma-mixing and crustal anatexis in sub-volcanic  
 1030 conduits. *Journal of Petrology*, **39**, 519-550.

1031 RAISWELL, R., BOTTRELL, S. H., AL-BIATTY, H. J. & TAN, M. M. 1993. The influence of bottom water  
 1032 oxygenation and reactive iron content on sulphur incorporation into bitumens from Jurassic  
 1033 marine shales. *American Journal of Science*, **293**, 569-596.

1034 RIPLEY, E. M. & LI, C. 2013. Sulphide saturation in mafic magmas: Is external sulphur required for  
 1035 magmatic Ni-Cu-(PGE) ore genesis? *Economic Geology*, **108**, 45-58.

1036 RIPLEY, E. M., LIGHTFOOT, P. C., LI, C. & ELSWICK, E. R. 2003. Sulphur isotopic studies of continental flood  
 1037 basalts in the Noril'sk region: implications for the association between lavas and ore-bearing  
 1038 intrusions. *Geochimica et Cosmochimica Acta*, **67**, 2805-2817.

1039 RIPLEY, E. M., PARK, Y.-R., LI, C. & NALDRETT, A. J. 1999. Sulphur and oxygen isotopic evidence of  
 1040 country rock contamination in the Voisey's Bay Ni-Cu-Co deposit, Labrador, Canada. *Lithos*,  
 1041 **47**, 53-68.

1042 ROBINSON, B. W. & KUSAKABE, M. 1975. Quantitative preparation of sulphur dioxide for  $^{34}\text{S}/^{32}\text{S}$  analyses  
 1043 from sulphides by combustion with cuprous oxide. *Analytical Chemistry*, **47**, 1179-1181.

1044 SACHS, P. M. & STANGE, S. 1993. Fast assimilation of xenoliths in magmas. *Journal of Geophysical*  
 1045 *Research*, **98**, 19741.

1046 SAUNDERS, A. D., FITTON, J. G., KERR, A. C., NORRY, M. J., *et al.* 1997. The North Atlantic Igneous  
 1047 Province. In: *Large Igneous Provinces: Continental, Oceanic, and Planetary Flood Volcanism*.  
 1048 (eds. MAHONEY, J. J. & COFFIN, M. F.), pp. 45-93. Washington DC: American Geophysical Union.

1049 SCHOFIELD, N. J., BROWN, D. J., MAGEE, C. & STEVENSON, C. T. 2012. Sill morphology and comparison of  
 1050 brittle and non-brittle emplacement mechanisms. *Journal of the Geological Society*, **169**,  
 1051 127-141.

1052 SHARMAN, E.R., PENNISTON-DORLAND, S.C., KINNAIRD, J.A., NEX, P.A.M., BROWN, M. AND WING, B.A. 2013  
1053 Primary origin of marginal Ni-Cu-(PGE) mineralization in layered intrusions:  $\Delta^{33}\text{S}$  evidence  
1054 from the Platreef, Bushveld, South Africa. *Economic Geology*, **108**, 365-377.

1055 SHAW, C. S. J. 2009. Caught in the act — The first few hours of xenolith assimilation preserved in lavas  
1056 of the Rockeskyllerkopf volcano, West Eifel, Germany. *Lithos*, **112**, 511-523.

1057 SIMKIN, T. 1967. Flow differentiation in the picritic sills of north Skye. In WYLLIE, P.J. (Ed.), *Ultramafic*  
1058 *and related rocks*. Wiley, New York.

1059 STEWART, A. D. 2002. *The Later Proterozoic Torridonian Rocks of Scotland: their sedimentology,*  
1060 *geochemistry and origin*, Geological Society, London.

1061 SVENSEN, H., PLANKE, S., MALTHER-SØRENSEN, A., JAMTVEIT, B., MYKLEBUST, R., EIDEM, T.R., REY, S.S. 2004.  
1062 Release of methane from a volcanic basin as a mechanism for initial Eocene global warming.  
1063 *Nature*, **429**, 542-545.

1064 SVENSEN, H., JAMTVEIT, B., PLANKE, S., CHEVALLIER, L. 2006. Structure and evolution of hydrothermal vent  
1065 complexes in the Karoo Basin, South Africa. *Journal of the Geological Society, London*, **163**,  
1066 671-682.

1067 SVENSEN, H., PLANKE, S., CHEVALLIER, L. MALTHER-SØRENSEN, A., CORFU, F., JAMTVEIT, B. 2007. Hydrothermal  
1068 venting of greenhouse gases triggering Early Jurassic global warming. *Earth and Planetary*  
1069 *Science Letters*, **256**, 554-566.

1070 SVENSEN, H., PLANKE, S., POLOZOV, A.G., SCHIDBAUER, N., CORFU, F., PODLADCHIKOV, Y.Y., JAMTVEIT, B. 2009.  
1071 Siberian gas venting and the end-Permian environmental crisis. *Earth and Planetary Science*  
1072 *Letters*, **277**, 490-500.

1073 SVENSEN, H., CORFU, F., POLTEAU, S., ØYVIND H., PLANKE, S. 2012. Rapid magma emplacement in the Karoo  
1074 Large Igneous Province. *Earth and Planetary Science Letters*, **325-326**, 1-9.

1075 THIRLWALL, M. F. & JONES, N. W. 1983. Isotope geochemistry and contamination mechanisms of Tertiary  
1076 lavas from Skye, NW Scotland. In: *Continental basalts and mantle xenoliths*. (eds.  
1077 HAWKESWORTH, C. J. & NORRY, M. J.), pp. 186-208. Nantwich: Shiva.



1078 THOMPSON, R. N. 1982. Magmatism of the British Tertiary Volcanic Province. *Scottish Journal of*  
1079 *Geology*, **18**, 49-107.

1080 THOMSON, K. & SCHOFIELD, N. 2008. Lithological and structural controls on the emplacement and  
1081 morphology of sills in sedimentary basins. *In*: THOMSON, K. & PETFORD, N. (eds) *Structure and*  
1082 *emplacement of high-level magmatic systems*. Geological Society, London, Special  
1083 Publication, **302**, pp. 31-44.

1084 THRASHER, J. 1992. Thermal effect of the Tertiary Cuillins Intrusive Complex in the Jurassic of the  
1085 Hebrides: an organic geochemical study. *In: Basins on the Atlantic Seaboard: Petroleum*  
1086 *Geology, Sedimentology and Basin Evolution*. (eds. PARNELL, J.), pp. 35-49.

1087 TORSSANDER, P. 1989. Sulphur isotope ratios of Icelandic rocks. *Contributions to Mineralogy and*  
1088 *Petrology*, **102**, 18-23.

1089 TUTTLE, M. L., GOLDBERGER, M. B. & WILLIAMSON, D. L. 1986. An analytical scheme for determining forms  
1090 of sulphur in oil shales and associated rocks. *Talanta*, **33**, 953-961.

1091 WAGNER, T., BOYCE, A. & FALICK, A. E. 2002. Laser combustion analysis of  $\delta^{34}\text{S}$  of sulfosalt minerals:  
1092 determination of the fractionation systematics and some crystal-chemical considerations.  
1093 *Geochimica et Cosmochimica Acta*, **66**, 2855-2863.

1094 WHITE, N. & LOVELL, B. 1997. Measuring the pulse of a plume with the sedimentary record. *Nature*,  
1095 **387**, 888-891.

1096 YALLUP, C., EDWARDS, M., TURCHYN, A.V. 2013. Sulphur degassing due to contact metamorphism during  
1097 flood basalt eruptions. *Geochimica et Cosmochimica Acta*, **120**, 263-279.

1098 ZHABINA, N. & VOLKOV, I. A method of determination of various sulphur compounds in sea sediments  
1099 and rocks. 3rd International Symposium on Environmental Biogeochemistry, 1978. Ann  
1100 Arbor Science Publications, 735-746.

1101

1102

1103

Fig. 1

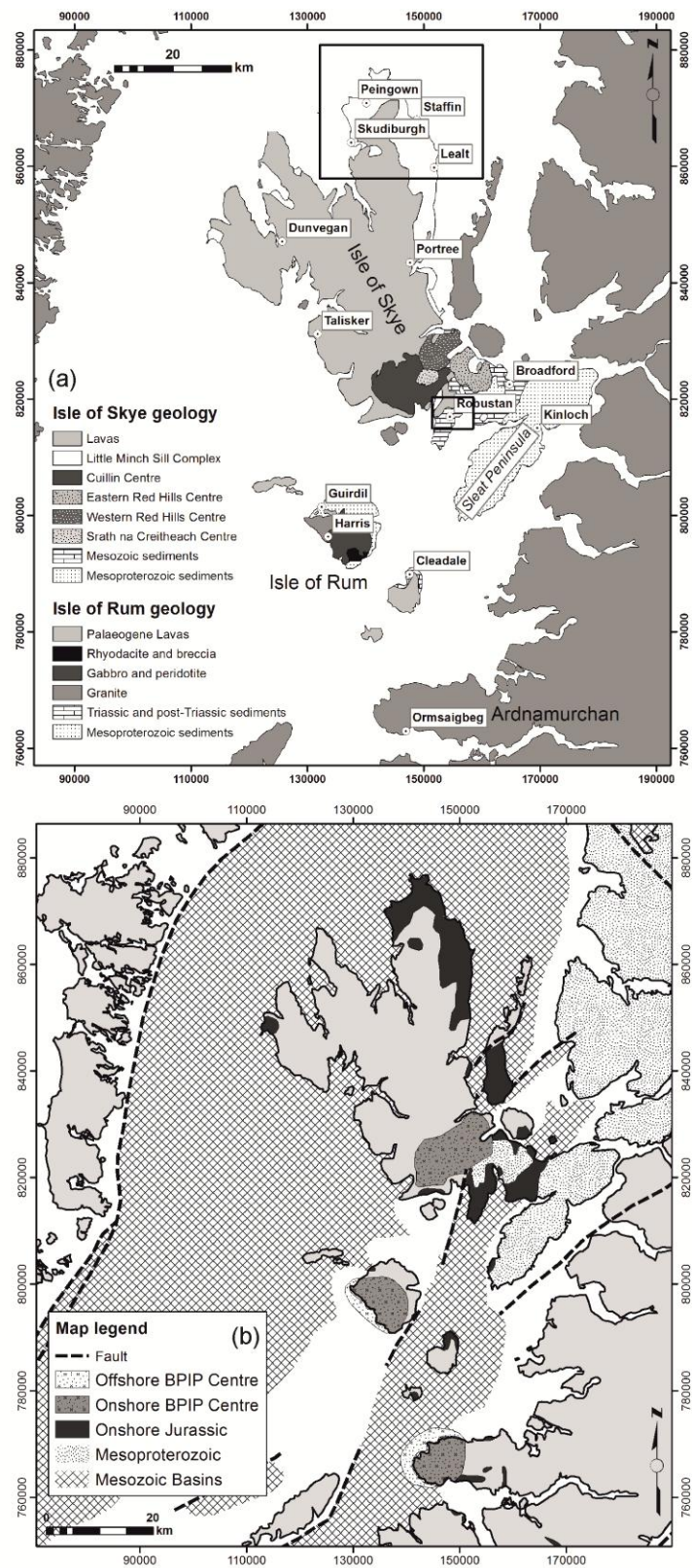


Fig. 2

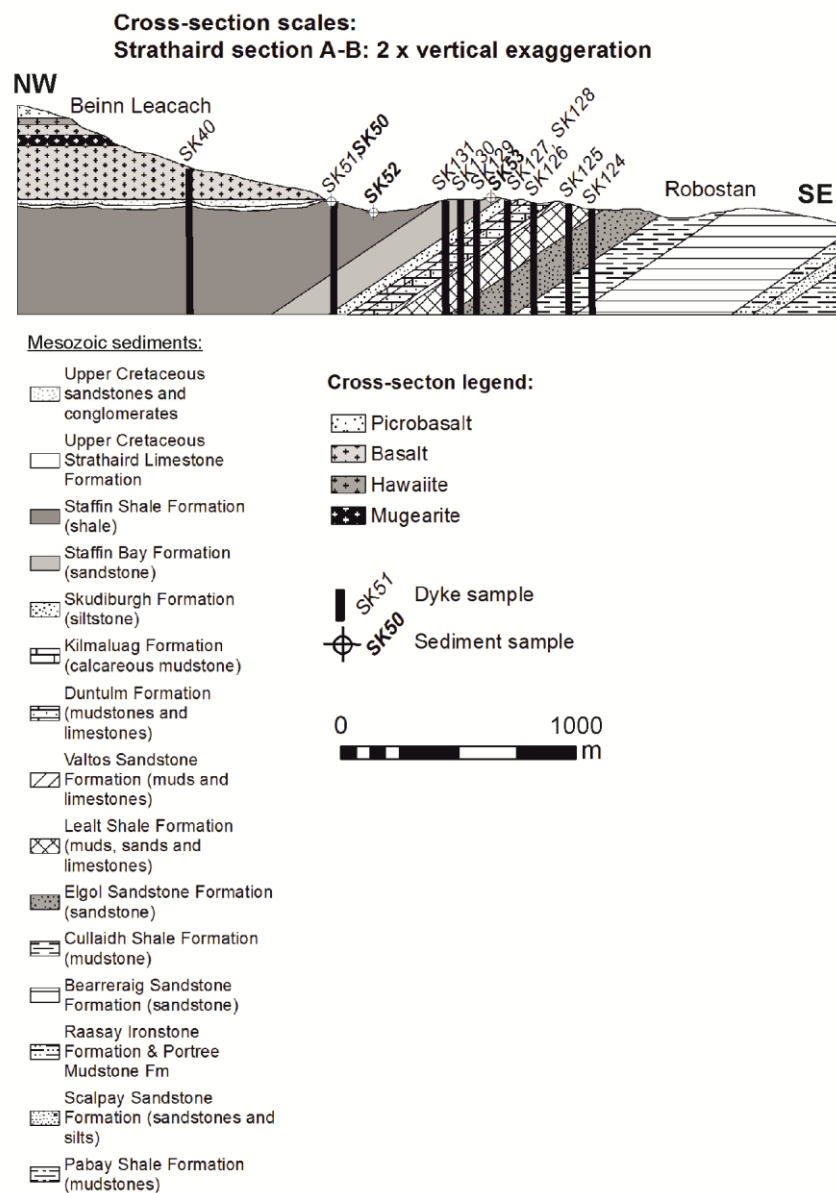




Fig. 3

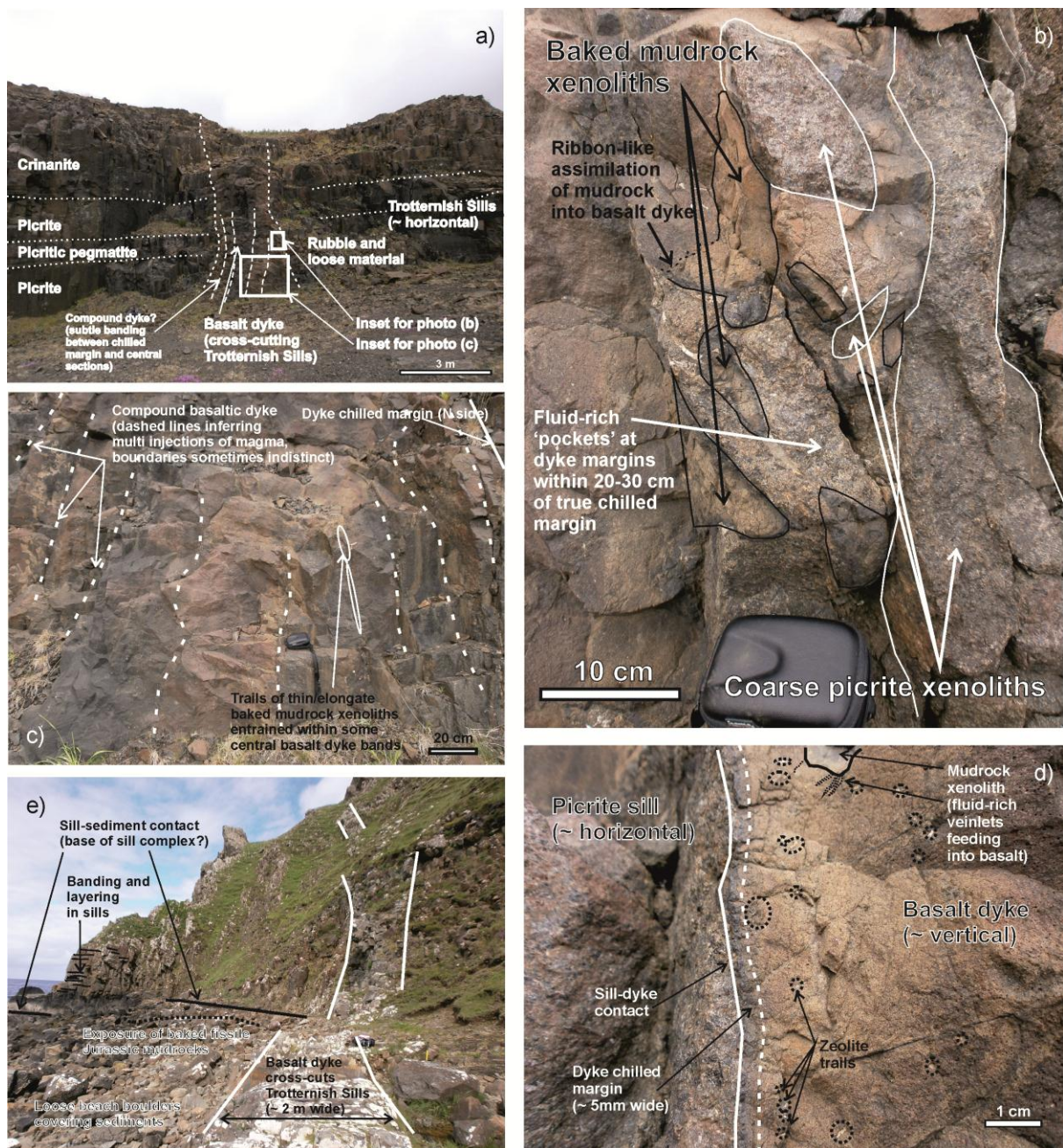


Fig. 4

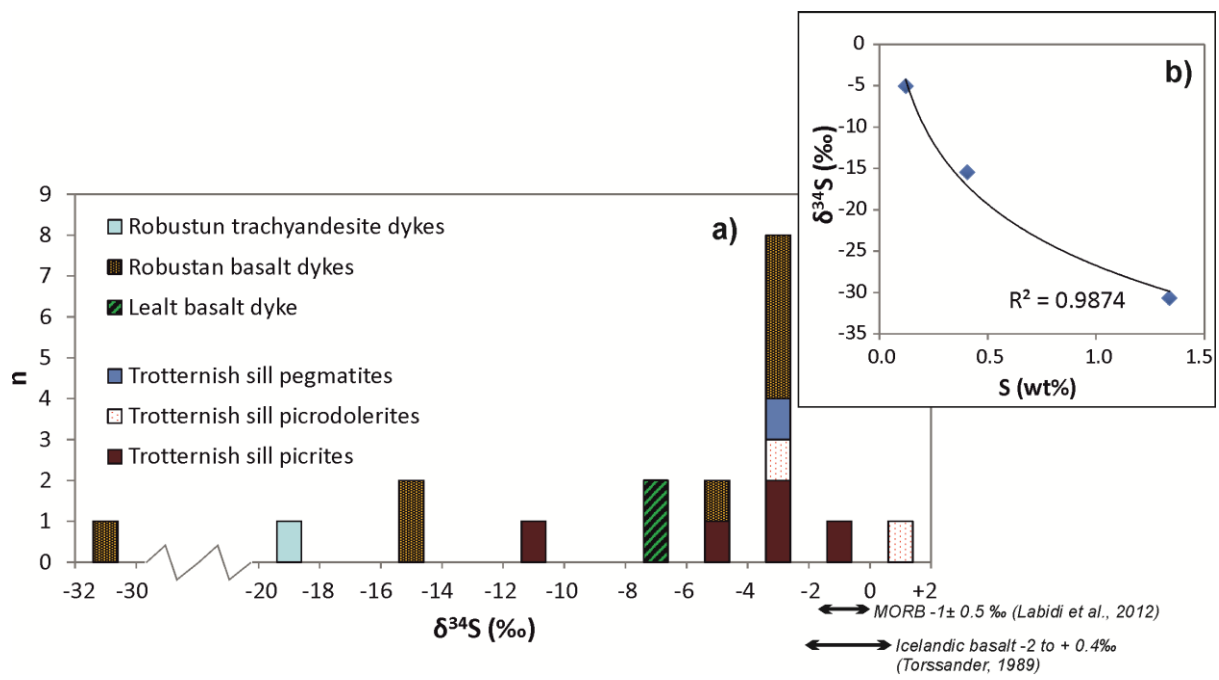


Fig. 5

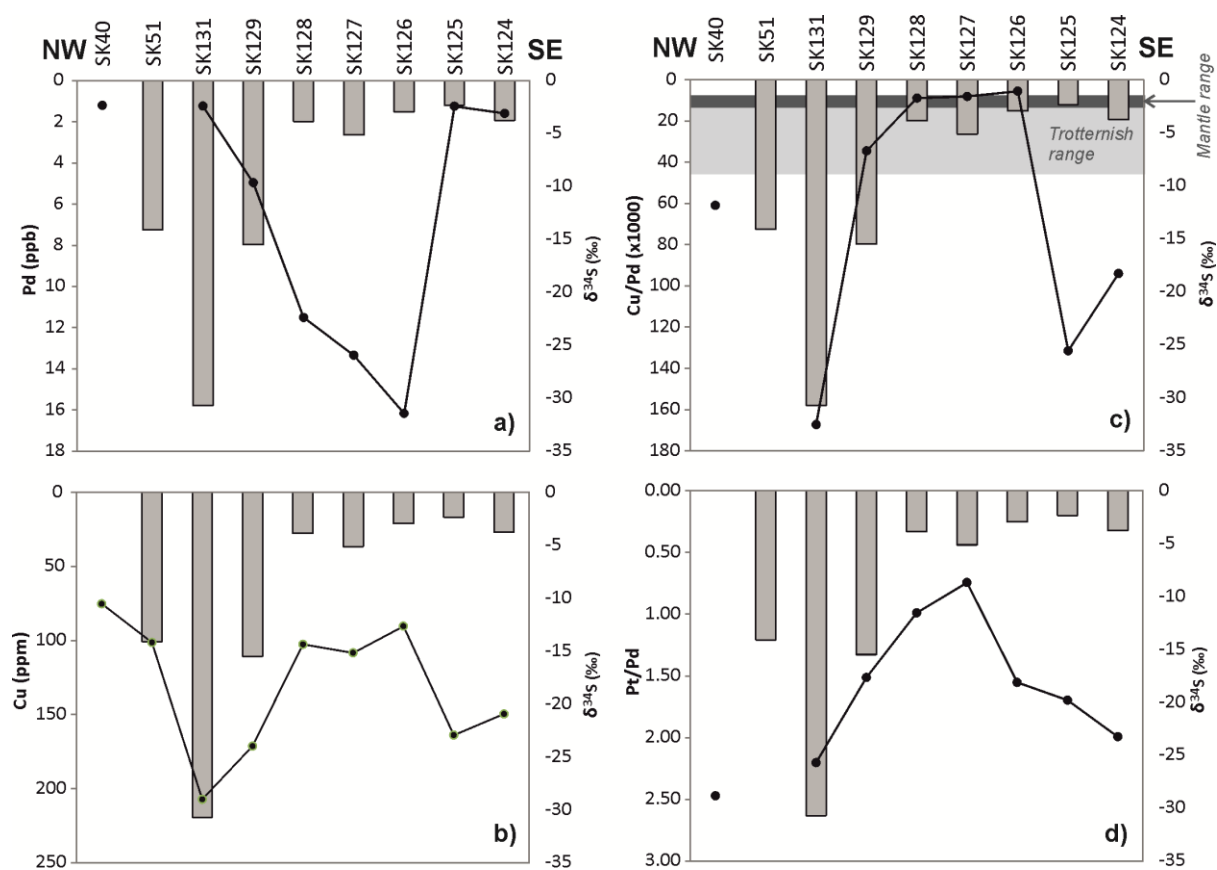


Fig. 6

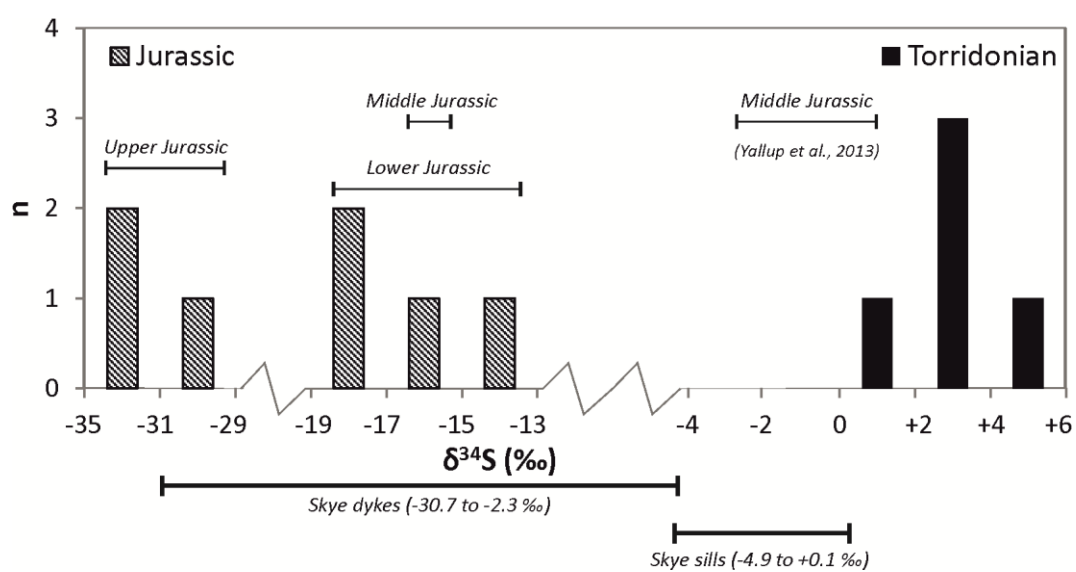


Fig. 7

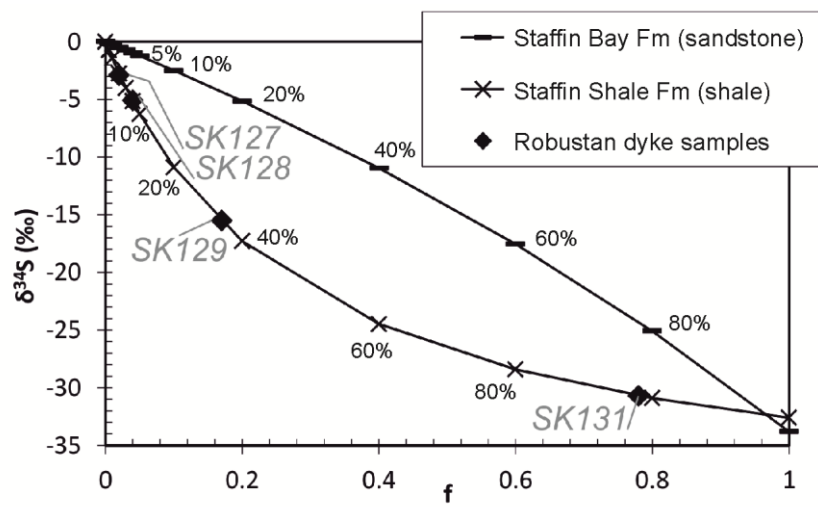
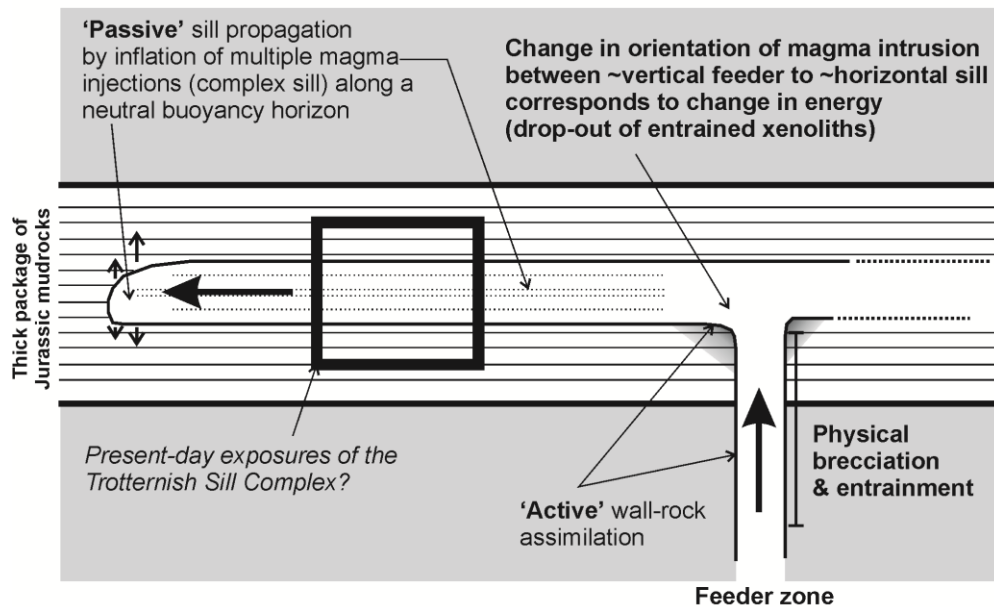




Fig. 8

a) 'Passive' intrusion for sills



b) 'Active' intrusion for dykes

